

DRAWDOWN MANAGEMENT STRATEGIES: MIDLAND BASIN CASE STUDIES

A Thesis

by

YOGASHRI UMESH PRADHAN

Submitted to the Office of Graduate and Professional Studies of
Texas A&M University
in partial fulfillment of the requirements for the degree of

MASTER OF SCIENCE

Chair of Committee, Thomas Blasingame
Co-Chair of Committee, Eduardo Gildin
Committee Members, Kan Wu
 Zenon Medina-Cetina
Head of Department, Jeffrey Spath

December 2020

Major Subject: Petroleum Engineering

Copyright 2020 Yogashri Pradhan

ABSTRACT

Operators have different production strategies based on maintaining their fracture networks to the reservoir and sand control after flowback. Aggressive production strategies in some liquids-rich producing shale reservoirs could reduce fracture lengths and limit the production life. In addition, operators are constantly trying to achieve a better understanding of the existing fracture network (*i.e.*, to assess if a perceived fracture barrier restricts the potential SRV or if modified drawdown strategies could make up for these "restricted" wells) to determine its impact on different production strategies. This study investigates optimal drawdown strategies through a holistic workflow. The scope of this work will also investigate what are the hydrocarbon recoveries for wells that are landed near a fracture barrier as well as primary-infill well scenarios.

The work considers important reservoir and fluid properties to conduct rate-transient analyses, pressure transient analyses, and later to develop the reservoir simulation model to history match and forecast future production rates and pressures. The study considers multiple scenarios of varying properties from fracture and reservoir modeling to obtain a range of recoveries and economics. Case studies will cover the Midland Basin Wolfcamp and Lower Spraberry formations to evaluate how reservoirs of different rock and fluid properties will impact the resulting optimal choke management strategies.

Coupled geomechanics and reservoir simulation is a recognized industry practice used to better understand potential fracture network depletion influenced by fracture barriers and primary-infill well scenarios, ultimately providing guidance on optimal drawdown strategies for complex reservoir development scenarios.

DEDICATION

To my family:

My parents Amarja and Umesh Pradhan — thank you for introducing me to engineering, your unconditional love, and support for everything I do.

My colleagues and managers at Endeavor Energy Resources.

My husband, Ryan Yarger for his love and support in all of my endeavors.

ACKNOWLEDGEMENTS

I would like to acknowledge:

Dr. Thomas A. Blasingame for his guidance, patience, and his expectations for his students to achieve excellence. No matter how intimidating his requirements are, the final product is something one can be proud of.

Dr. Eduardo Gildin for his patient teaching and for always being there for his students. He taught me much about reservoir simulation, and for that effort I am most appreciative.

Endeavor Energy Resources for supporting my graduate education and providing the data for this study.

CONTRIBUTORS AND FUNDING SOURCES

Contributors

This work was supervised by a thesis committee consisting of Dr. Thomas Blasingame, Dr. Eduardo Gildin, and Dr. Kan Wu of the Department of Petroleum Engineering and Dr. Zenon Medina-Cetina of the Department of Civil Engineering.

Funding Sources

Graduate study was the candidate's employer, Endeavor Energy Resources. The contents of this thesis are solely the responsibility of the authors and do not necessarily represent the official views of the Texas A&M Department of Petroleum Engineering nor Endeavor Energy Resources.

TABLE OF CONTENTS

	Page
CHAPTER 1 INTRODUCTION AND LITERATURE REVIEW	
1.1 Objectives	1
1.2 Statement of the Problem	1
1.3 Workflow.....	5
1.4 Deliverables.....	6
1.5 Organization of Thesis	7
CHAPTER 2 DECLINE CURVE ANALYSIS	
2.1 Orientation to Decline Curve Analysis	9
2.2 Discussion of Results	18
CHAPTER 3 RATE TRANSIENT ANALYSIS	
3.1 Orientation to Rate Transient Analysis	21
3.2 Discussion of Results	30
CHAPTER 4 PRESSURE TRANSIENT ANALYSIS	
4.1 Orientation to Pressure Transient Analysis	32
4.2 Discussion of Results	37
CHAPTER 5 NUMERICAL MODELING	
5.1 Orientation to Numerical Modeling	38
5.2 Numerical Modeling Cases	41
5.3 Discussion of Results	46
CHAPTER 6 FRACTURE MODELING	
6.1 Orientation to Fracture Modeling	49
6.2 Discussion of Results	50
CHAPTER 7 SUMMARY, CONCLUSIONS, AND RECOMMENDATIONS	
7.1 Summary	52
7.2 Conclusions	52
7.3 Recommendations	54
NOMENCLATURE	55
REFERENCES	56

LIST OF FIGURES

	Page
Figure 1.1 — Workflow to Determine Optimal Drawdown Strategies for Wells Near a Fracture Barrier and Primary-Infill Well Scenarios.	5
Figure 2.1 — Well 1 Production History	10
Figure 2.2 — Well 2 Production History	10
Figure 2.3 — Well 3 Production History	11
Figure 2.4 — Well 4 Production History	11
Figure 2.5 — Well 5 Production History	12
Figure 2.6 — Well 6 Production History	12
Figure 2.7 — Well 7 Production History	13
Figure 2.8 — Well 8 Production History	13
Figure 2.9 — Well 9 Production History	14
Figure 2.10 — Well 10 Production History	14
Figure 2.11 — Well 11 Production History	15
Figure 2.12 — Well 12 Production History	15
Figure 2.13 — Well 13 Production History	16
Figure 2.14 — Well 14 Production History	16
Figure 2.15 — Well 15 Production History	17
Figure 2.16 — Gun Barrel View of Case Studies	19
Figure 3.1 — Well 1 Linear Flow Plot (with RTA model imposed)	23
Figure 3.2 — Well 2 Linear Flow Plot (with RTA model imposed)	23
Figure 3.3 — Well 3 Linear Flow Plot (with RTA model imposed)	24
Figure 3.4 — Well 4 Linear Flow Plot (with RTA model imposed)	24
Figure 3.5 — Well 5 Linear Flow Plot (with RTA model imposed)	25

Figure 3.6	—	Well 6 Linear Flow Plot (with RTA model imposed)	25
Figure 3.7	—	Well 7 Linear Flow Plot (with RTA model imposed)	26
Figure 3.8	—	Well 8 Linear Flow Plot (with RTA model imposed)	26
Figure 3.9	—	Well 9 Linear Flow Plot (with RTA model imposed)	27
Figure 3.10	—	Well 10 Linear Flow Plot (with RTA model imposed)	27
Figure 3.11	—	Well 11 Linear Flow Plot (with RTA model imposed)	28
Figure 3.12	—	Well 12 Linear Flow Plot (with RTA model imposed)	28
Figure 3.13	—	Well 13 Linear Flow Plot (with RTA model imposed)	29
Figure 3.14	—	Well 14 Linear Flow Plot (with RTA model imposed)	29
Figure 3.15	—	Well 15 Linear Flow Plot (with RTA model imposed)	30
Figure 4.1	—	Well 2 Log-Log Plot (with PTA model imposed)	34
Figure 4.2	—	Well 4 Log-Log Plot (with PTA model imposed)	34
Figure 4.3	—	Well 5 Log-Log Plot (with PTA model imposed)	35
Figure 4.4	—	Well 7 Log-Log Plot (with PTA model imposed)	35
Figure 4.5	—	Well 8 Log-Log Plot (with PTA model imposed)	36
Figure 4.6	—	Well 9 Log-Log Plot (with PTA model imposed)	36
Figure 4.7	—	Well 11 Log-Log Plot (with PTA model imposed)	37

Figure 5.1 — Configuration of Upper and Lower Wolfcamp A Wells	39
Figure 5.2 — Configuration of Wolfcamp B Wells.....	39
Figure 5.3 — Cumulative Oil Production Results for the Wolfcamp B Wells	45
Figure 5.4 — Gas-Oil-Ratio (GOR) Trends from Numerical Modelling Cases	48

LIST OF TABLES		Page
Table 2.1	— Oil EUR Results and Landing Zone for Each Well Studied	18
Table 3.1	— Standard Parameter Assumptions for the Analytical Reservoir Model	21
Table 3.2	— Pressure and Reservoir Thickness Constraints for Cases Studies	21
Table 3.3	— Rate Transient Analysis Results for Selected Wells in This Work	22
Table 4.1	— Maximum Values Possible for Various Parameters	33
Table 4.2	— Results comparisons — PTA and RTA	33
Table 5.1	— General Reservoir Properties	38
Table 5.2	— Post History Match Drawdown Strategies for Primary-Infill Scenario	41
Table 5.3	— Post-History Match Drawdown Strategies for Primary-Infill Well Scenario ..	42
Table 5.4	— Post History Match Drawdown Strategy for Co-Developed Cases	43
Table 5.5	— Post History Match Drawdown Strategy for Co-Developed Cases	43
Table 5.6	— Post History Match Drawdown Strategies for Well Near Fracture Barrier	44
Table 6.1	— Fracture Model Properties	49
Table 6.2	— Computed Fracture Heights	50

CHAPTER 1

INTRODUCTION AND LITERATURE REVIEW

1.1 Objectives

The main objectives of this work are to:

- Investigate wells with at least six months of production data.
- Conduct unconventional reservoir diagnostics to compare well performance.
- Understand fracture propagation and ultimate recoveries of the base case from simulation.
- Understand the effects of different (pressure) drawdown strategies from simulation.

1.2 Statement of The Problem

All operators have different production and recovery objectives, which results in varied recommendations for (pressure) drawdown strategies. However, the industry needs to develop a better understanding of the geomechanics, geology, and development history of the area of interest.

Decline Curve Analyses (DCA)

Internal practices for forecasting well performance consider:

- Selection of wells of interest for a type well curve
- Fitting a modified hyperbolic decline curve relationship to the type well curve
- Conducting economics based upon a 30-year well life and internal cost structure

Time-rate analysis, or decline curve analysis, is a standard method used to estimate reserves in unconventional reservoirs, which is why this work includes this analysis as a comparison to rate-transient analysis and simulation results. A shortcoming of time-rate analysis is the assumption of a constant flowing bottomhole pressure throughout the life of the well. It is well-recognized that there is a significant period of variability in the flowing bottomhole pressure history over the life of wells producing from unconventional reservoirs. In addition, using a conservative choke

management strategy (*i.e.*, slowly changing the choke size until its full diameter), production will result in shallow declines, which could delay production forecasting or hinder the certainty of time-rate analysis results (Collins et al 2014).

Rate Transient and Pressure Transient Analyses (RTA and PTA)

Wilson and Alla (2017) suggest that a rate-time pressure analysis (RTA) model can be developed based on the expected hydraulic fracture geometries and reservoir properties for targets of interest. A match for rate and pressure data will be performed to estimate the initial, average reservoir pressure for each well of interest. A change in closure stress as the reservoir depletes is also critical information to combine with the matched average reservoir pressure. Closure stress is dependent on the pore pressure drop defined by:

$$\Delta\sigma_{closure} = \alpha \frac{(1 - 2\nu)}{(1 - \nu)} \Delta p_p$$

Where α is Biot's constant, ν is Poisson's ratio, and Δp_p is the change in pore pressure.

Wilson and Alla also mention that the key output from the RTA model is the average reservoir pressure over time, which will be used to predict the changing stress conditions inside the stimulated rock volume (SRV). Results from the RTA workflow and sensitivity analyses pertinent to the research will be fracture half-lengths (x_f), SRV permeability (k_{SRV}), effective thickness (h), and fracture conductivity (F_{CD}) (Lerza et al 2018). These parameters could then be used as thresholds (*i.e.* achieving a certain value for fracture conductivity to achieve optimal EUR's) to influence future drawdown strategies, or drawdown (psi/hr) (Wilson and Alla 2017).

Pressure-transient tests in industry relating to drawdown management are primarily taken from the diagnostic fracture injection test (DFIT). Wang and Sharma (2018) mention that pressure-transient

data after shut-in from a DFIT provides in-situ stresses, fracture treatment design parameters, and reservoir properties.

Numerical Methods with Reservoir and Geomechanics Properties

Kumar et al (2018) compare aggressive versus conservative drawdown management strategies on the effect of fracture conductivity using a fully coupled geomechanical reservoir simulator. They found that unpropped fractures close when the drawdown is increased, sealing a large portion of the fracture network. The optimal choke management strategy depends on the sensitivity of the fracture conductivity to stress. Additionally, a conservative drawdown strategy will yield a higher cumulative production for targets that have fracture conductivities sensitive to stress (higher clay content). An aggressive drawdown strategy could close those fractures and limit well production.

Wilson et al (2016) compare aggressive versus conservative drawdown strategies and well log-calibrated geomechanics and reservoir simulation models to evaluate the optimal drawdown strategies in the Midland Basin. The coupled geomechanics-reservoir modeling incorporates sensitivities of different drawdown rates for the Wolfcamp B. The Wilson et al study concluded that to avoid proppant damage and reduce produced water handling costs, at the expense of lower EUR predictions, a conservative drawdown (1-2 psi/hr) strategy (choke management over a period of months) is the optimal strategy for the Wolfcamp B.

Fracture Barrier Identification

Shelokov et al (2017) examine the relationship between Poisson's Ratio, Young's Modulus, and lithology in the context of the capability to fracture by defining fracture facies for wells in the Midland Basin Wolfcamp. The Shelokov et al work discusses what would be/should be considered a fracture barrier and how to identify optimal landing points in Wolfcamp A and B. For instance, the Wolfcamp A and B intervals show a "thinly-bedded" response on the gamma ray log consisting

of carbonate and carbonate-rich shale "layers." The authors suggest this is a sequence of high depositional cycles where cyclic alteration happens on the scale of 2 ft. or less. Well log data from more than 1500 vertical wells were analyzed for the purpose of mapping the reservoir properties (Shelokov et al 2017). For the scope of this research, observations and practices from the literature will be applied to well log data in order to determine fracture barriers.

Primary-Infill Well Impacts

Wang et al (2019) present key observations from real-time bottomhole pressure gauge data and used these data to develop mechanistic models to optimize drawdown strategy in the DOE-HFTS area. This comprehensive dataset provides a better understanding on the role that geomechanics plays in field development of unconventional reservoirs, and how age differences between the primary and infill wells in the Upper and Middle Wolfcamp affect pressure drawdown strategies and ultimate recoveries.

Crespo and Cuervo differentiates drawdown management and choke management strategies as separate concepts because drawdown management strategies focus on the importance of flowing bottomhole pressures and normalizes the effect of how much fluid and proppant is pumped per lateral foot. Reservoirs which are susceptible to fracture conductivity damage due to pressure drawdown make drawdown strategies significant. Additionally, drawdown strategies will be different when pore pressure and geomechanical properties are different (*e.g.*, for primary-infill scenarios).

1.3 Workflow

Figure 1.1 illustrates the workflow developed for this study to establish optimal drawdown strategies for two complex development scenarios — 1-wells considered near a fracture barrier and 2-primary-infill well scenarios. The optimal pressure drawdown strategy is considered to be the strategy which yields the most recovery (hence, value) for the wells of interest.'

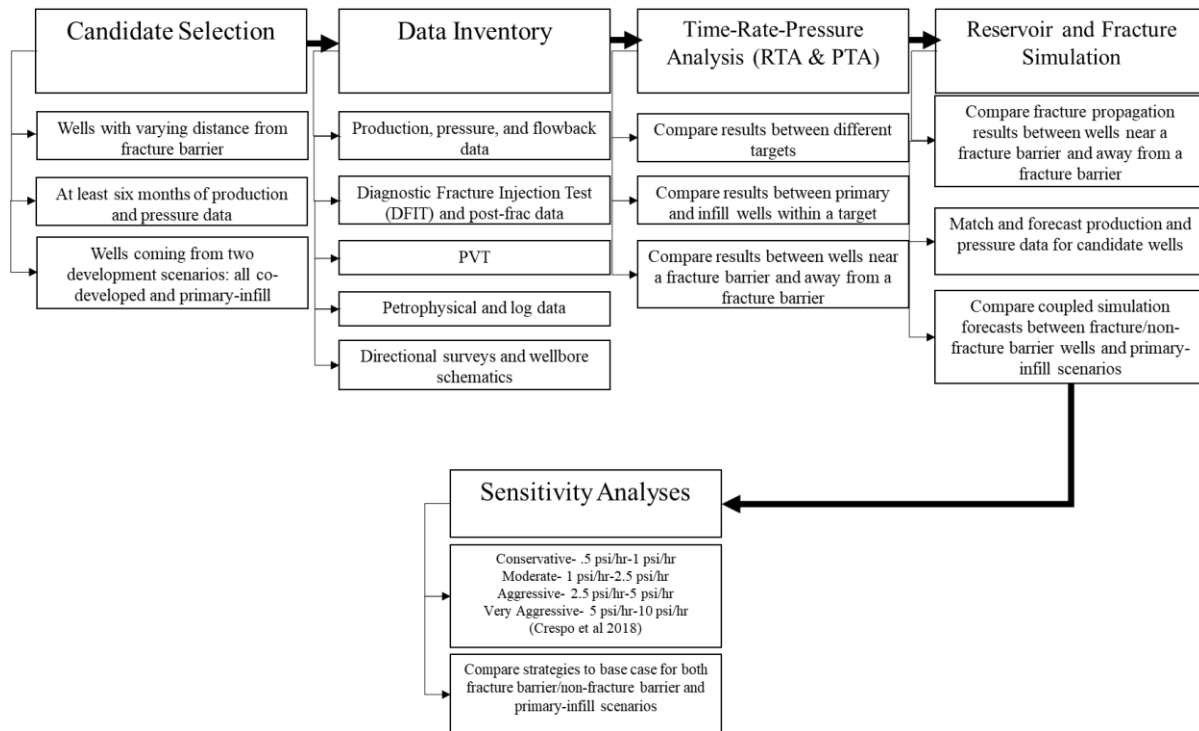


Figure 1.1 — Workflow to Determine Optimal Drawdown Strategies for Wells Near a Fracture Barrier and Primary-Infill Well Scenarios.

1.4 Deliverables

The primary goal of this work is to evaluate the influence of increased pressure drawdown with the goal of maximizing oil recovery for the following cases:

- Wells completed and produced at the same time.
- Wells which have a fracture barrier between vertically adjacent landing points.
- Wells that have primary-infill relationships laterally and vertically from each other.

The proposed deliverables of this work are:

- To create an inventory of wells with > 6 months of production history in order to:
 - Establish wells which may have landed near to or far from a fracture barrier.
 - Establish wells which may have direct fracture interactions.
 - Create a comprehensive database of reservoir, completion, flowback, and production data.
- To perform rate-transient analyses (RTA), pressure transient analyses (PTA), and decline curve analyses (DCA) as appropriate to:
 - Identify any specific "fracture-driven interactions" (or frac-hits).
 - Identify well-to-well/regional pressure depletion (*i.e.*, well interference).
 - Identify specific flow regime features relevant to assessment of well/fracture interference.
 - Estimate model parameters used for PTA and RTA.
 - Estimate the ultimate recovery for a given well using standard DCA methods.
 - Identify correlations between wells that have landed near a fracture barrier.
- To perform reservoir simulation study(s) appropriate in depth and scope to:
 - Understand the reservoir behavior due to the created hydraulic fracture system.
 - Understand the relevance/significance of a fracture network (impact on offset wells).
 - Predict the well and reservoir performance of single and multiwell configurations.
 - (time and data permitting) Incorporate geomechanics into the reservoir modelling.
- To use the reservoir modeling and historical choke strategies for selected wells to:
 - Review prior drawdown strategies to assess various strategies on well performance.
 - Develop optimal drawdown strategies for the specific field cases considered.

1.5 Organization of Thesis

This thesis is organized as follows:

- Chapter 1 — Introduction and Literature Review
 - Objectives
 - Statement of the Problem
 - Workflow
 - Deliverables
 - Organization of Thesis
- Chapter 2 — Decline Curve Analysis
 - Orientation to Decline Curve Analysis
 - Discussion of Results
- Chapter 3 — Rate Transient Analysis
 - Orientation to Rate Transient Analysis
 - Discussion of Results
- Chapter 4 — Pressure Transient Analysis
 - Orientation to Rate Transient Analysis
 - Discussion of Results
- Chapter 5 — Numerical Modeling
 - Orientation to Numerical Modeling
 - Numerical Modeling Cases
 - Discussion of Results
- Chapter 5 — Fracture Modeling
 - Orientation to Fracture Modeling
 - Discussion of Results

- Chapter 8 — Summary, Conclusions, Recommendations
 - Summary
 - Conclusions
 - Recommendations
- References
- Nomenclature

CHAPTER 2

DECLINE CURVE ANALYSIS

2.1 Orientation to Decline Curve Analysis

Wells with pressure and production data of at least six months were selected for decline curve analysis. From the inventory of wells provided, this led to fifteen wells being selected. These data are presented in **Figs. 2.1-2.15** along with the "modified-hyperbolic" decline curve analysis equation fitted to a given dataset. We note that a "terminal (exponential) decline" of 6 percent was used in all cases as this is an average of such values typically considered. Well data with shut-in periods were excluded in the analysis.

For reference, the "modified-hyperbolic" equation (a "splice" of Arps' hyperbolic relation with a "terminal" exponential relation is given by:

$$q(t) = \left\{ \begin{array}{ll} q_{i,\text{hyp}} \frac{1}{[1 + bD_i t]^{1/b}} & (t < t_{\text{lim}}) \\ q_{\text{lim}} \exp[-D_{\text{lim}} (t - t_{\text{lim}})] & (t > t_{\text{lim}}) \end{array} \right\} \quad \text{where} \quad \begin{array}{l} q_{\text{lim}} = q_{i,\text{hyp}} \left[\frac{D_{\text{lim}}}{D_i} \right]^{(1/b)} \\ t_{\text{lim}} = \frac{1}{bD_i} \left[\left[\frac{q_{i,\text{hyp}}}{q_{\text{lim}}} \right]^b - 1 \right] \end{array}$$

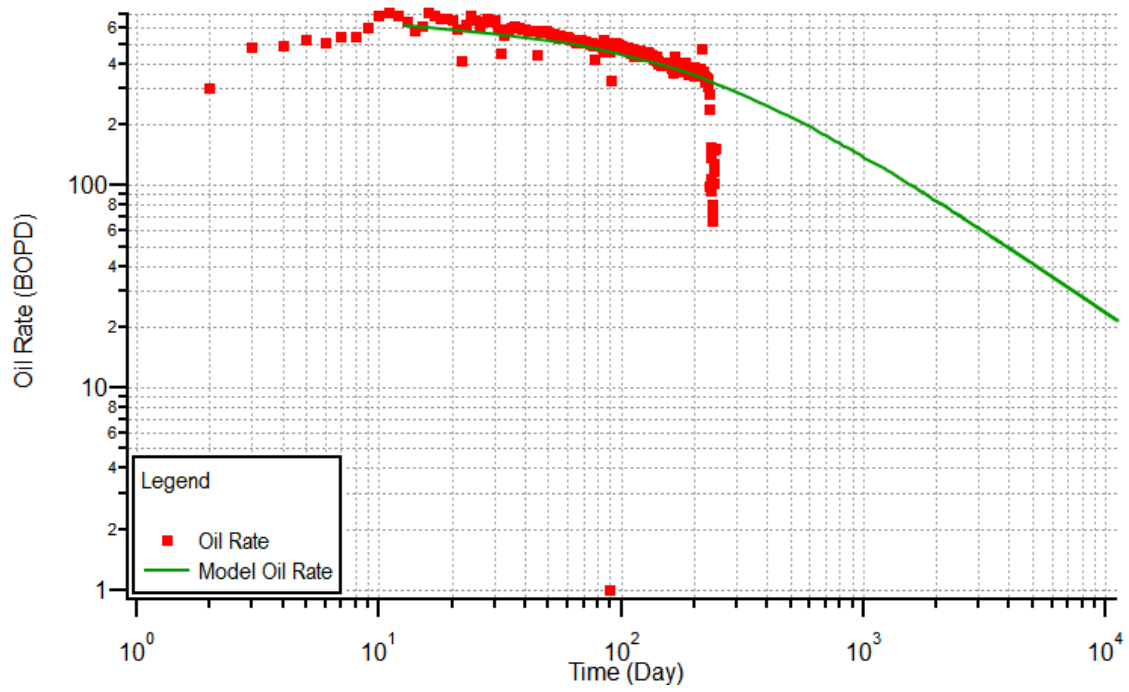


Figure 2.1 — Well 1 Production History.

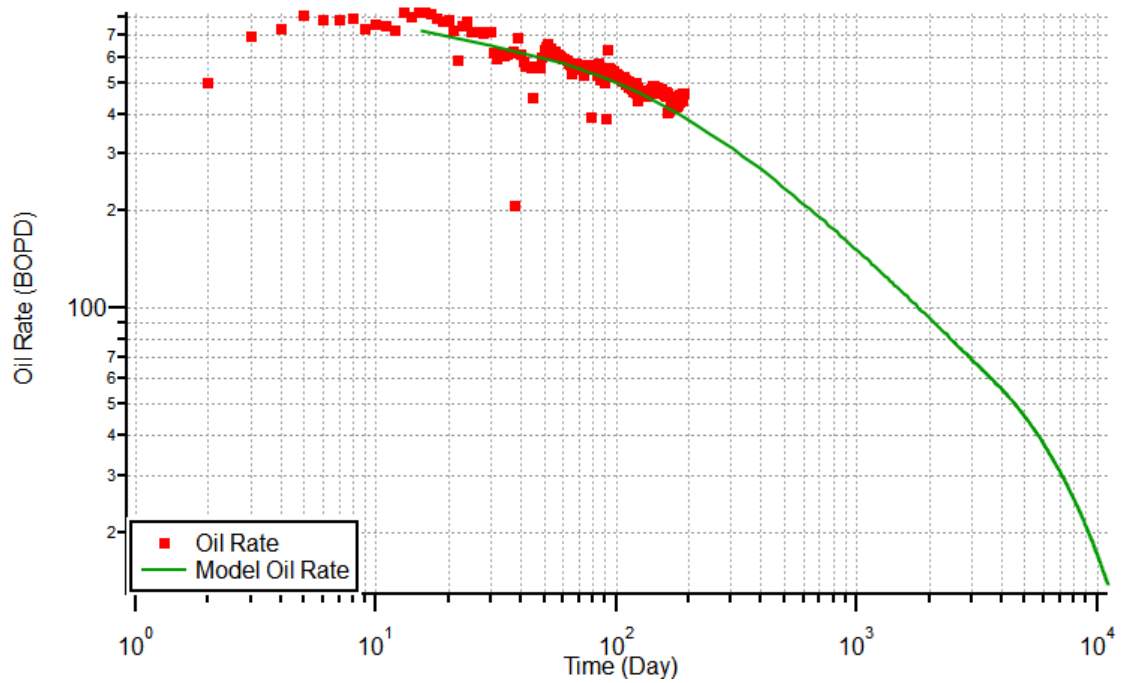


Figure 2.2 — Well 2 Production History.

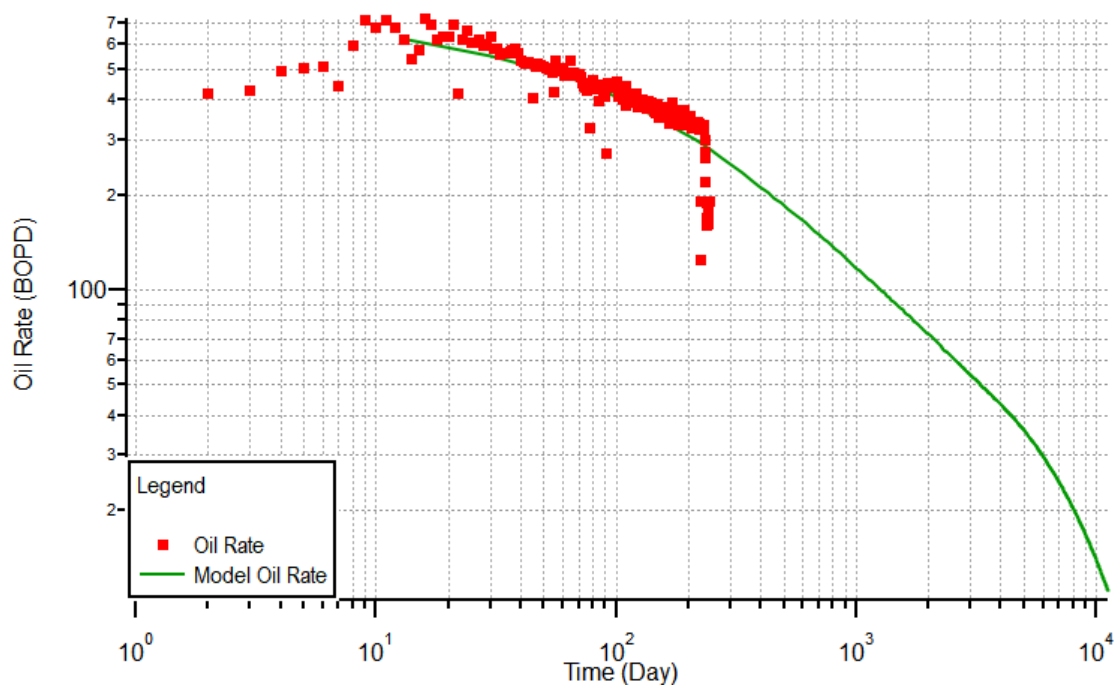


Figure 2.3 — Well 3 Production History.

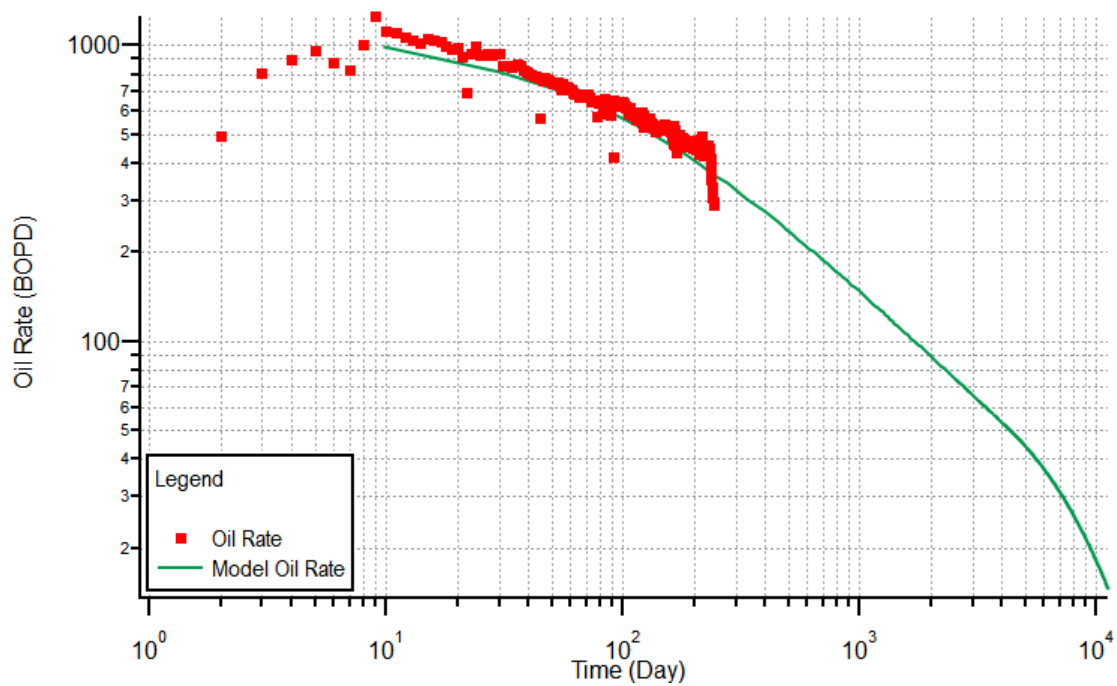


Figure 2.4 — Well 4 Production History.

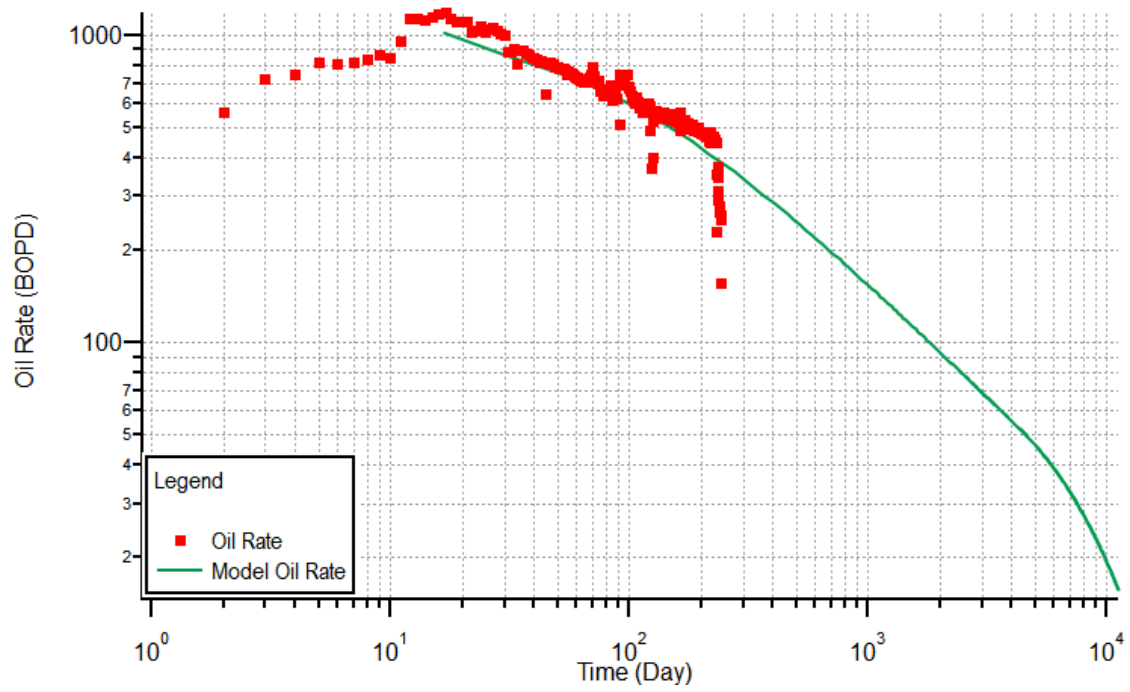


Figure 2.5 — Well 5 Production History.

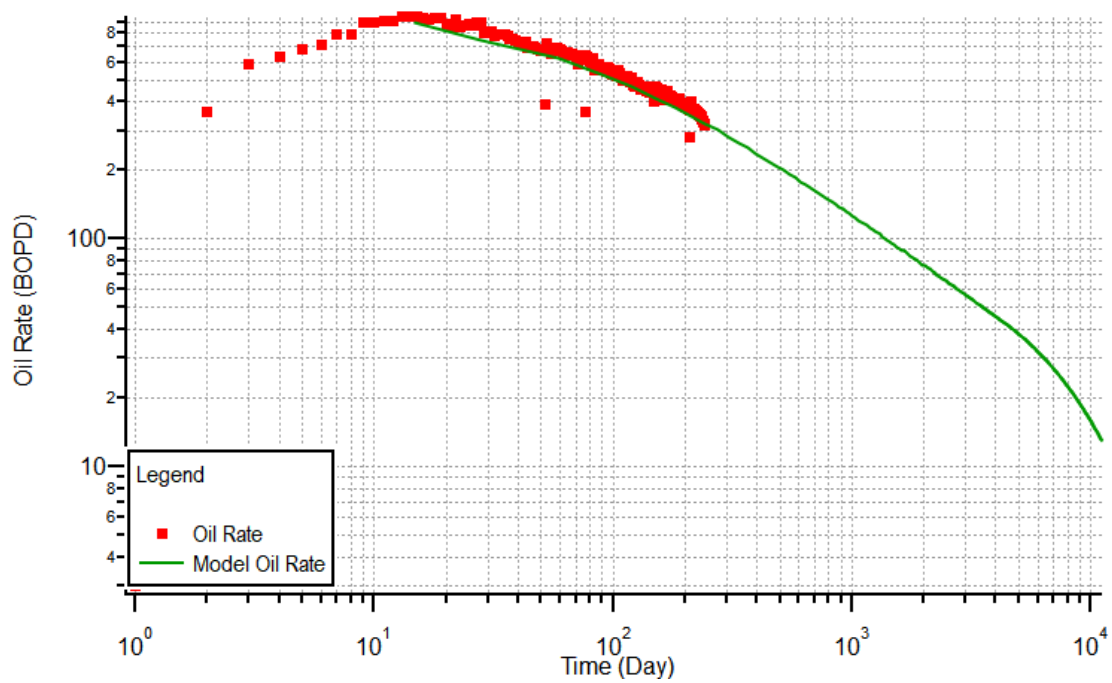


Figure 2.6 — Well 6 Production History.

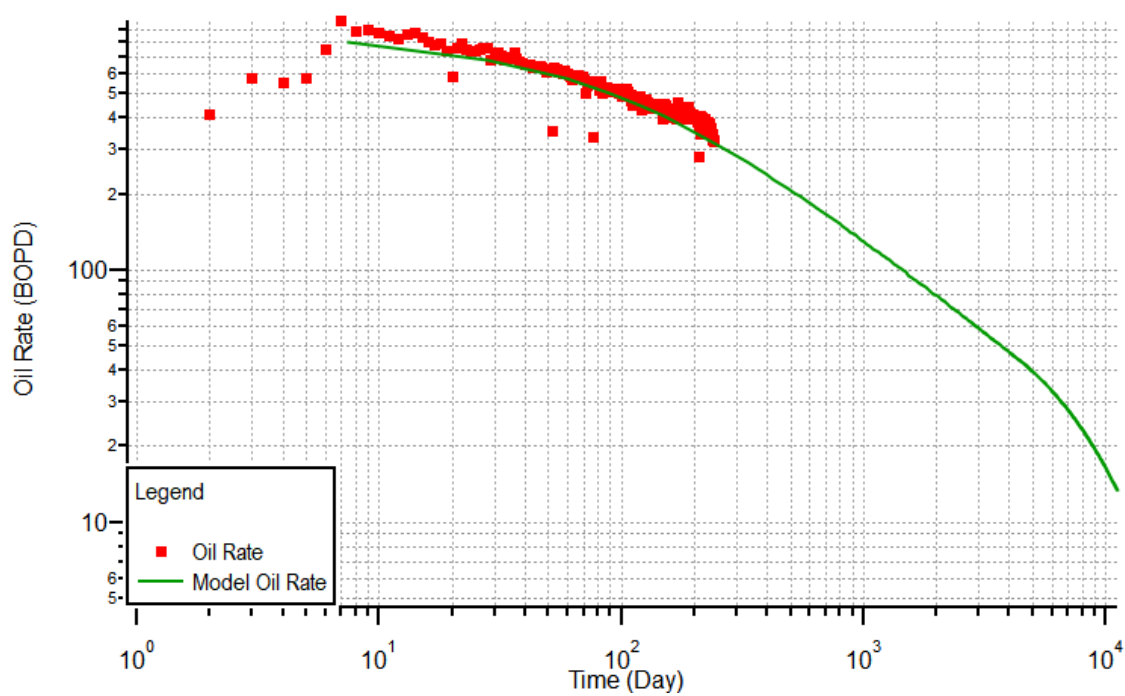


Figure 2.7 — Well 7 Production History.

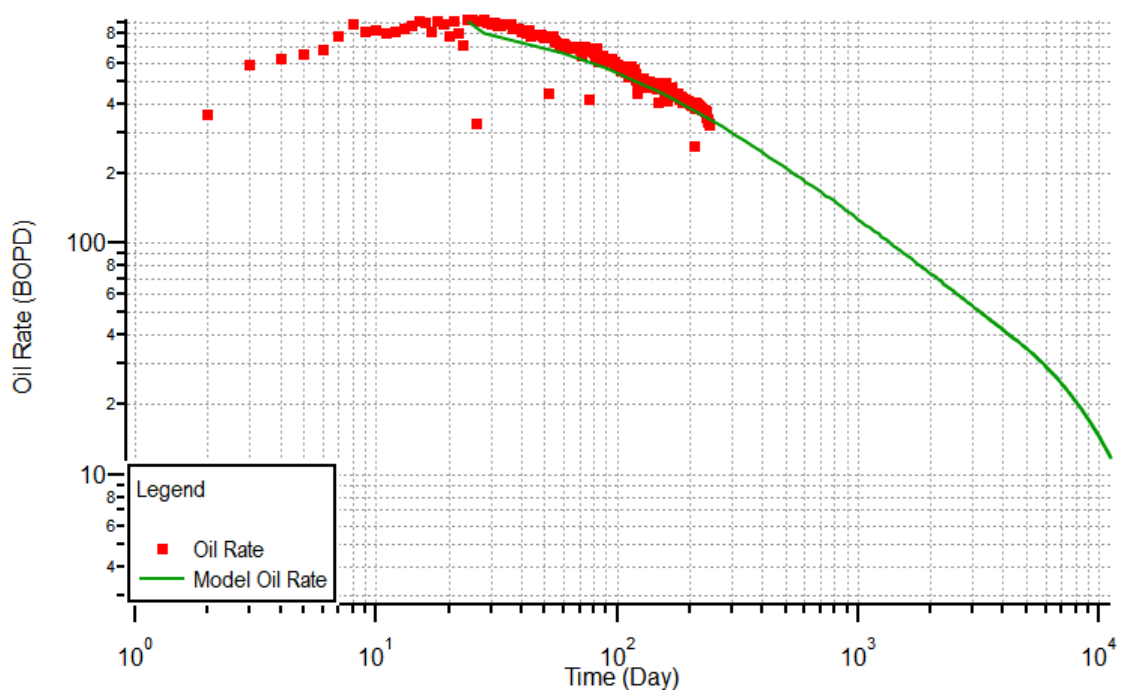


Figure 2.8 — Well 8 Production History.

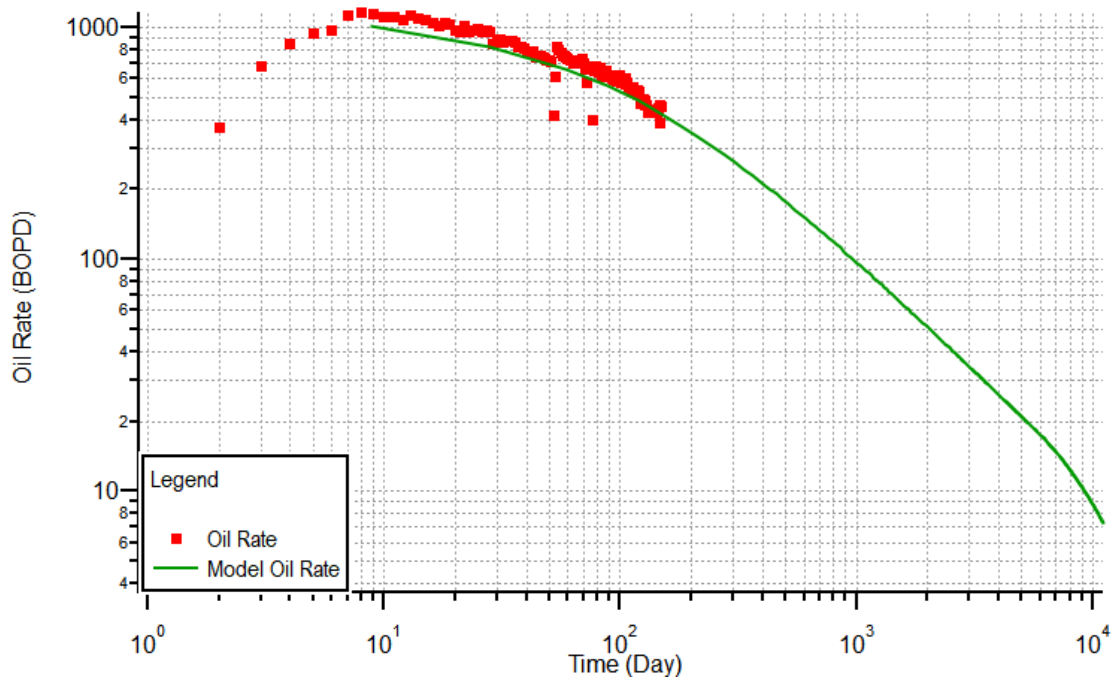


Figure 2.9 — Well 9 Production History.

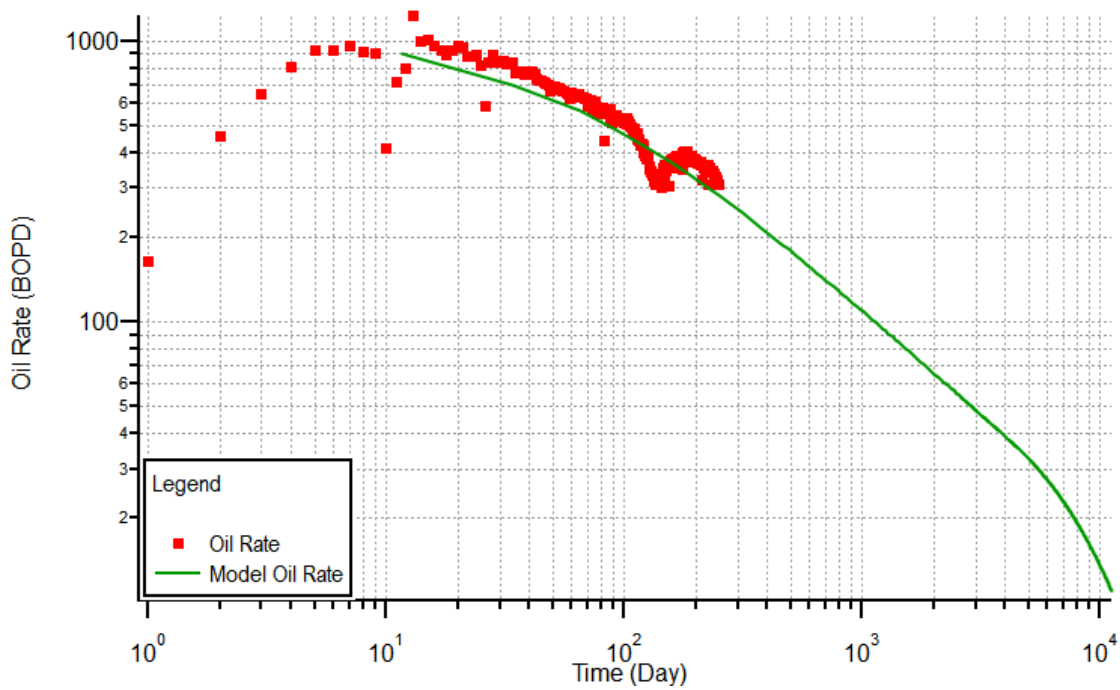


Figure 2.10 — Well 10 Production History.

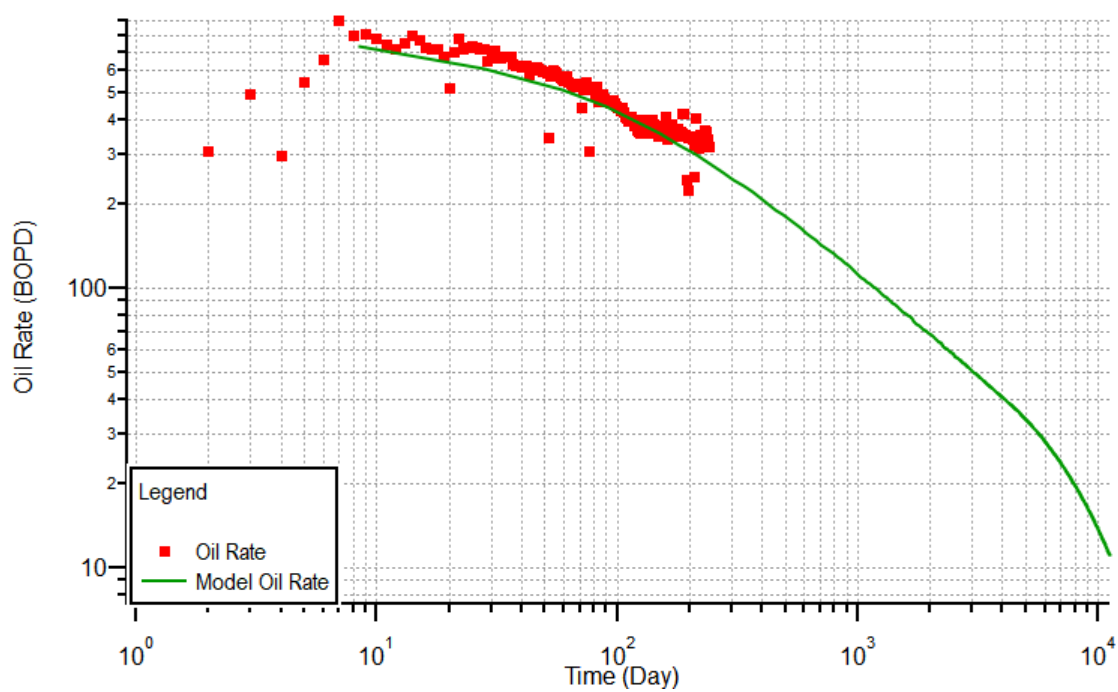


Figure 2.11— Well 11 Production History.

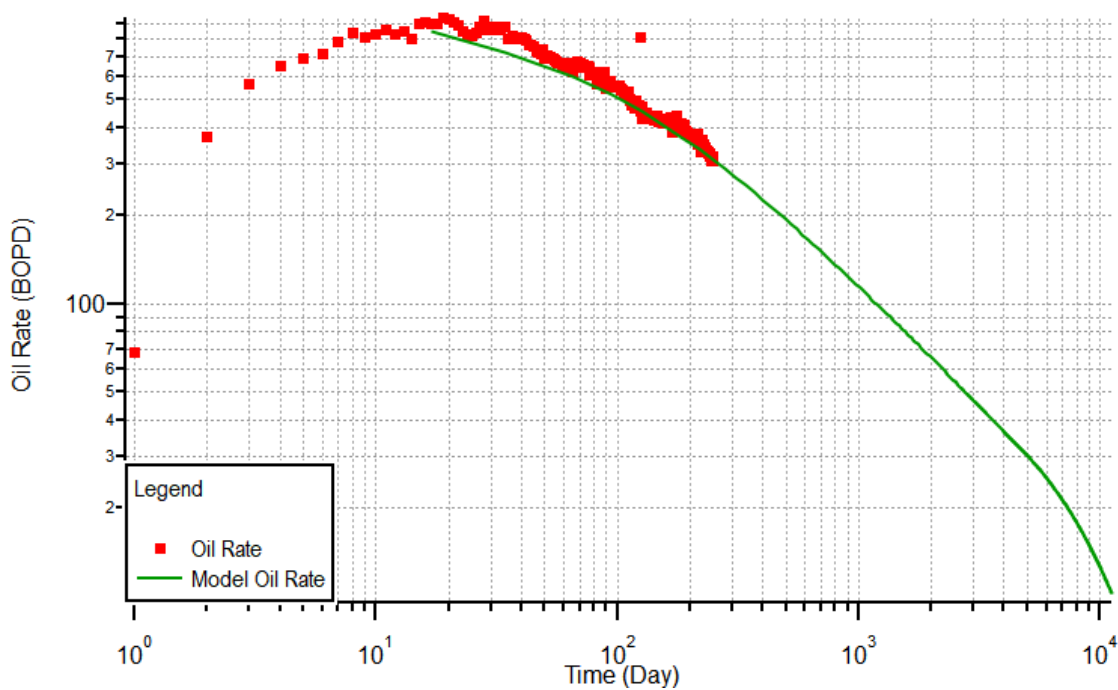


Figure 2.12— Well 12 Production History.

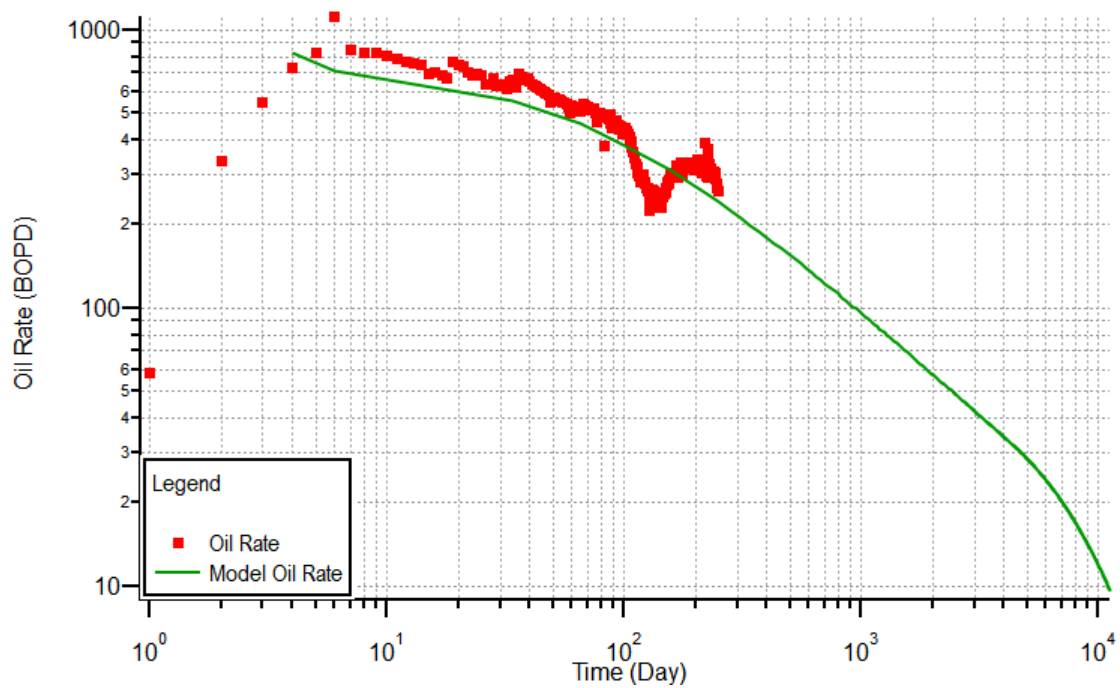


Figure 2.13— Well 13 Production History (Primary-Infill Well Interference).

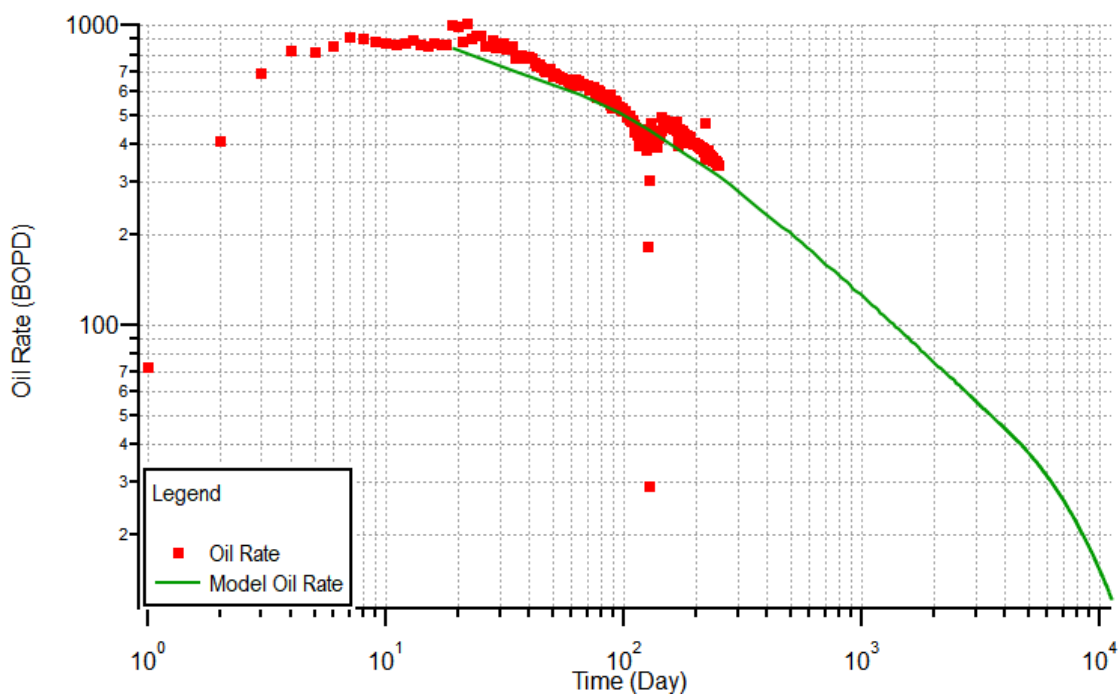


Figure 2.14— Well 14 Production History (Primary-Infill Well Interference).

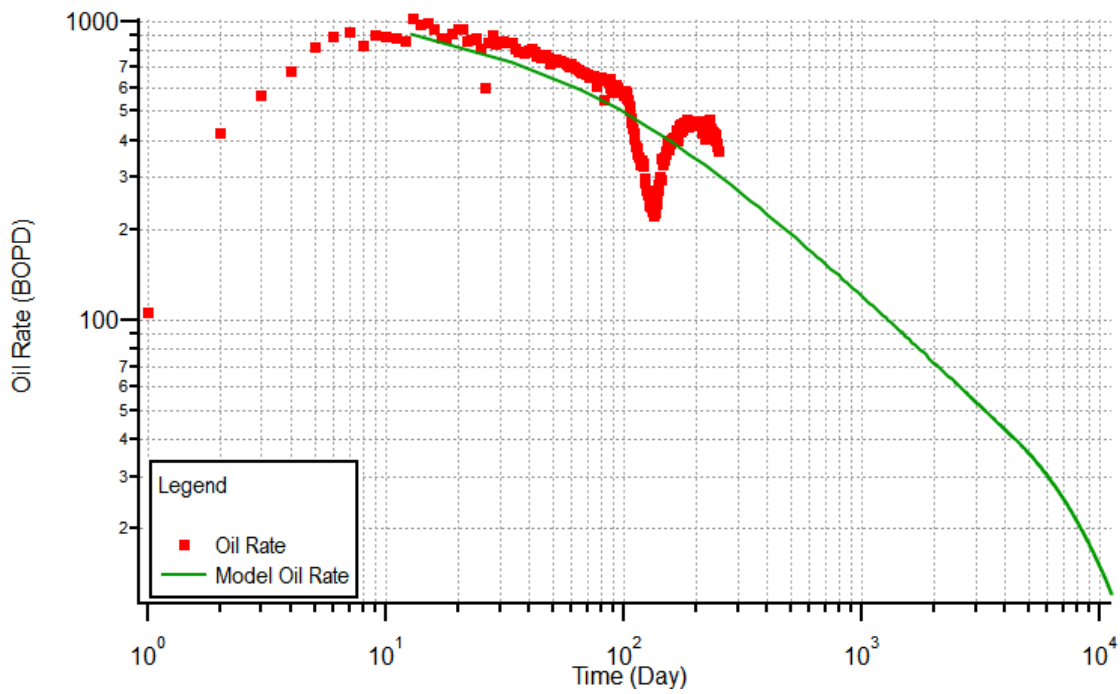


Figure 2.15— Well 15 Production History (Primary-Infill Well Interference).

As noted above, the modified-hyperbolic with and exponential terminal decline rate of 6 percent was used for all decline curve analysis cases. A commercial software package (Citrine — Kappa Engineering) was used for this work (specifically the green trendlines shown on **Figs. 2.1-2.15**).

2.2 Discussion of Results

In **Table 2.1** we present the results of the decline curve analysis (specifically the 30 year EUR). Each (coded) well number is given, along with "landing zone" in which the horizontal portion of the well was placed.

Table 2.1 — Oil EUR Results and Landing Zone for Each Well Studied.

Well	Landing Zone	Oil EUR MBO)
1	Upper Wolfcamp (Top)	724
2	Middle Wolfcamp	768
3	Upper Wolfcamp (Bottom)	608
5	Middle Wolfcamp	780
4	Upper Wolfcamp (Top)	819
6	Middle Wolfcamp	678
7	Upper Wolfcamp (Bottom)	684
8	Middle Wolfcamp	665
9	Upper Wolfcamp (Top)	509
10	Upper Wolfcamp (Top)	665
11	Upper Wolfcamp (Bottom)	592
12	Middle Wolfcamp	598
13	Upper Wolfcamp (Bottom)	514
14	Middle Wolfcamp	665
15	Upper Wolfcamp (Top)	647

Figure 2.16 provides a "gun-barrel" view (*i.e.*, a side view looking in the reservoir, directly in the well path) of the well configurations for the wells used in this study.

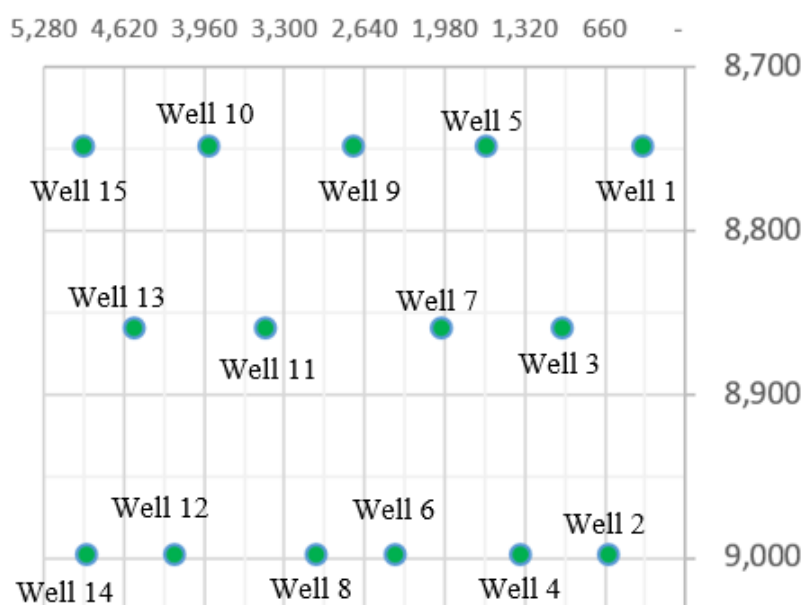


Figure 2.16— Gun-Barrel View of Case Studies.

It is believed that Well 2 is the well most affected by offset depletion from a competitor's development that had been producing four months prior. Wells 13, 14 and 15 were also affected by a competitor, except in these cases, Wells 13, 14 and 15 are the primary wells and the offset competitor's wells are the infill wells.

From **Table 2.1**, we note that wells which are landed in the lower portion of Wolfcamp A have lower EUR's due to the small vertical distance between the Upper Wolfcamp A and the Upper Wolfcamp B ($\approx 100'$). With all wells being on gas-lift, it is believed that the upper Wolfcamp A wells are converging to higher minimum flowing bottomhole pressures than the Wolfcamp B wells (data not shown in this section). This behavior suggests that a more aggressive pressure drawdown strategy is possible, which would result in proportionally higher production rates and recoveries.

Although the impact of the traditional assumptions for decline curve analysis cannot be assessed, we should mention that conventional decline-curve analysis assumes that boundary-dominated flow existed (for the terminal production decline) and that the operating conditions do not change (*i.e.*, the well is maintained at a constant flowing bottomhole pressure). Both of these assumptions are violated — however; in concept, the "modified-hyperbolic" with a terminal exponential decline does impose the "boundary-dominated" condition (with the operative word being impose). Despite these assumptions, we believe that the decline curve analyses performed in this work are relevant and reasonably accurate.

CHAPTER 3

RATE TRANSIENT ANALYSIS

3.1 Orientation to Rate Transient Analysis

For the rate transient analysis work, a single-phase, black-oil reservoir model was assumed. The model configuration and universal reservoir parameters are stated in **Table 3.1**. The pressure and reservoir thickness constraints are given (per well) in **Table 3.2**.

Table 3.1 — Standard Parameter Assumptions for the Analytical Reservoir Model.

Well	Horizontal fractured
Reservoir	Homogeneous
Boundary	Infinite
Upper Wolfcamp Pi (Top, psi)	5144
Upper Wolfcamp Pi (Bottom, psi)	5705
Middle Wolfcamp Pi (psi)	5949

Table 3.2 — Pressure and Reservoir Thickness Constraints for Cases Studies.

Well	Landing Zone	Min BHP (psi)	Last BHP Month	Minimum Pay Thickness	Maximum Pay Thickness
1	Upper Wolfcamp (Top)	2200	Aug-19	250	300
2	Middle Wolfcamp	1800	Aug-19	250	300
3	Upper Wolfcamp (Bottom)	1400	Oct-19	250	300
5	Middle Wolfcamp	1800	Aug-19	250	300
4	Upper Wolfcamp (Top)	2000	Aug-19	250	300
6	Middle Wolfcamp	2700	Aug-19	250	300
7	Upper Wolfcamp (Bottom)	1900	Dec-19	250	300
8	Middle Wolfcamp	1500	Dec-19	250	300
9	Upper Wolfcamp (Top)	2300	Dec-19	250	300
10	Upper Wolfcamp (Top)	1400	Dec-19	250	300
11	Upper Wolfcamp (Bottom)	1600	Dec-19	250	300
12	Middle Wolfcamp	1400	Dec-19	250	300
13	Upper Wolfcamp (Bottom)	2000	Dec-19	250	300
14	Middle Wolfcamp	3000	Dec-19	250	300
15	Upper Wolfcamp (Top)	1900	Dec-19	250	300

For reference, the data in **Table 3.2** are based on prior knowledge of the reservoir properties and the geological setting and structure. After obtaining an RTA match for each well, the wells were forecasted for 30 years to estimate the oil EUR on a per well basis. For reference, the flowing bottomhole pressure used for forecasting was the pressure at the last non-zero flowrate.

The rate transient analysis results are displayed in Table 3.3, where the fracture half-length (x_f) and Oil EUR (MBO) are highlighted as the primary results from rate transient analysis.

Table 3.3 — Rate Transient Analysis Results for Selected Wells in This Work.

Well	Landing Zone	x_f (ft)	h (ft)	k (md)	kh (md-ft)	Porosity (fraction)	Skin Factor	Oil EUR (MBO)
1	Upper Wolfcamp (Top)	300	299.53	4.24E-06	1.27E-03	0.06	2.80E-05	559
2	Middle Wolfcamp	81.19	300.31	6.36E-06	1.91E-03	0.06	5.13E-05	331
3	Upper Wolfcamp (Bottom)	183.01	300.00	3.99E-06	9.56E-04	0.06	3.04E-05	452
5	Middle Wolfcamp	83.27	299.06	7.65E-06	2.30E-03	0.06	2.87E-05	332
4	Upper Wolfcamp (Top)	200.31	292.94	4.94E-06	1.48E-03	0.06	2.20E-05	492
6	Middle Wolfcamp	150.24	280.00	9.00E-06	2.25E-03	0.06	1.09E-05	366
7	Upper Wolfcamp (Bottom)	147.62	245.06	4.61E-06	1.27E-03	0.06	2.24E-05	351
8	Middle Wolfcamp	78.96	238.62	7.82E-06	2.36E-03	0.06	2.85E-05	299
9	Upper Wolfcamp (Top)	187.26	262.14	5.14E-06	1.54E-03	0.06	1.93E-05	358
10	Upper Wolfcamp (Top)	180.95	276.32	4.29E-06	1.17E-03	0.06	2.21E-05	456
11	Upper Wolfcamp (Bottom)	113.71	250.00	4.58E-06	1.37E-03	0.06	1.99E-05	316
12	Middle Wolfcamp	82.81	283.02	6.89E-06	1.95E-03	0.06	3.80E-05	352
13	Upper Wolfcamp (Bottom)	113.97	273.13	4.54E-06	1.24E-03	0.06	1.95E-05	284
14	Middle Wolfcamp	100	299.72	7.14E-06	2.14E-03	0.06	3.99E-05	201
15	Upper Wolfcamp (Top)	225.46	276.32	4.20E-06	1.19E-03	0.06	2.36E-05	484

The rate transient analyses (RTA) work was performed in a commercial software package (Topaze — Kappa Engineering) — and the "linear flow" plots for each well are presented in **Figs. 3.1-3.15**.

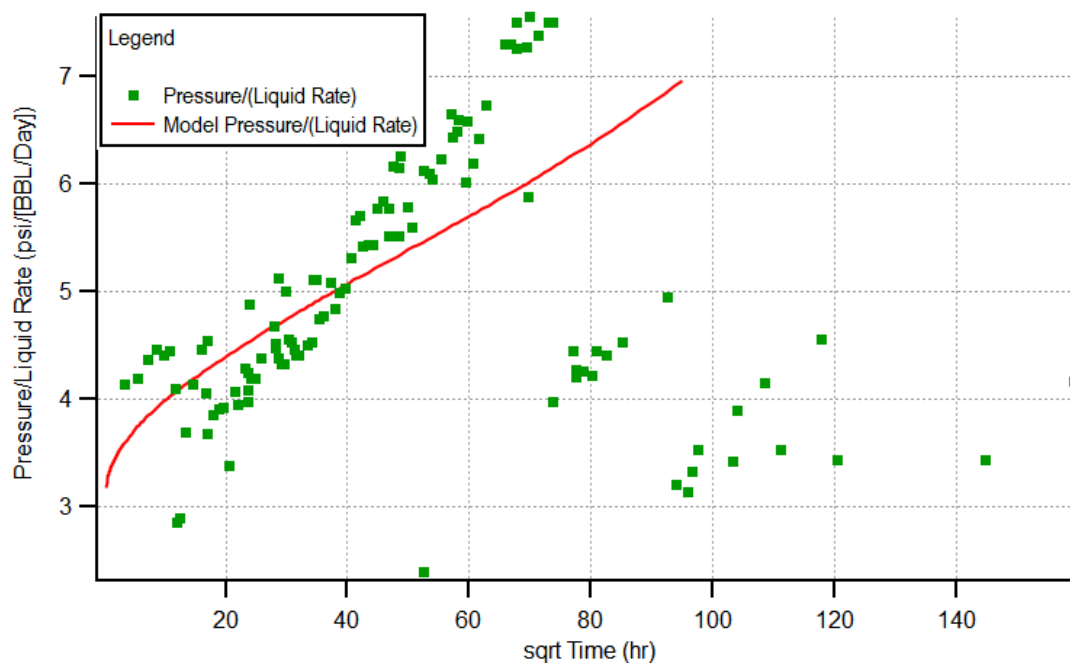


Figure 3.1 — Well 1 Linear Flow Plot (with RTA model imposed)

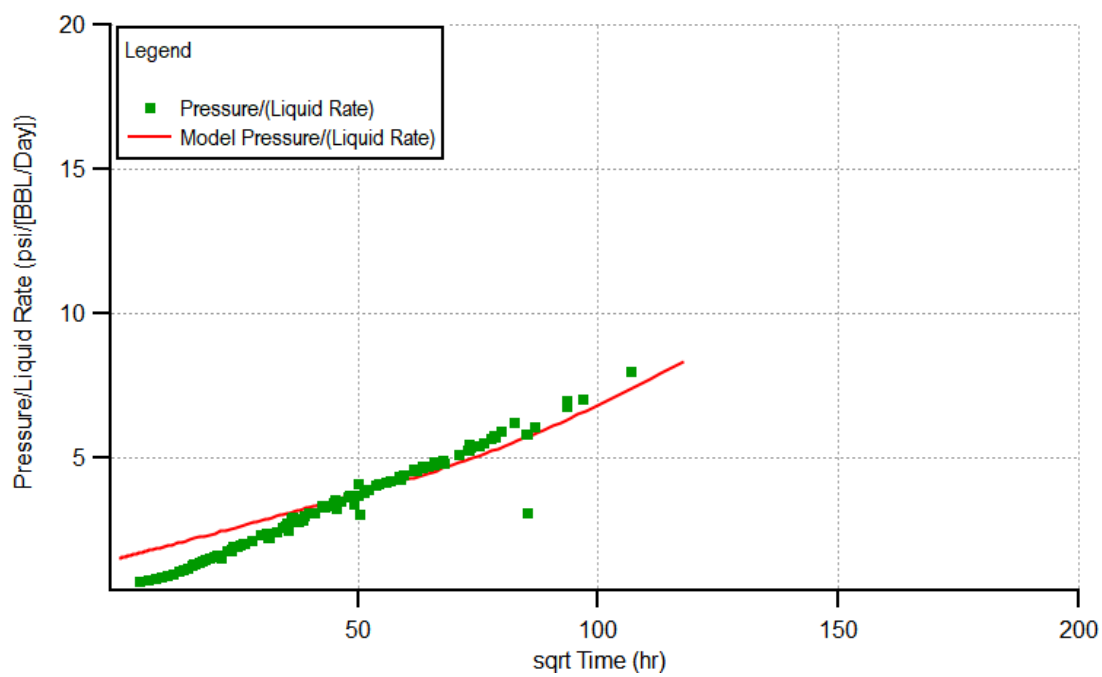


Figure 3.2 — Well 2 Linear Flow Plot (with RTA model imposed)

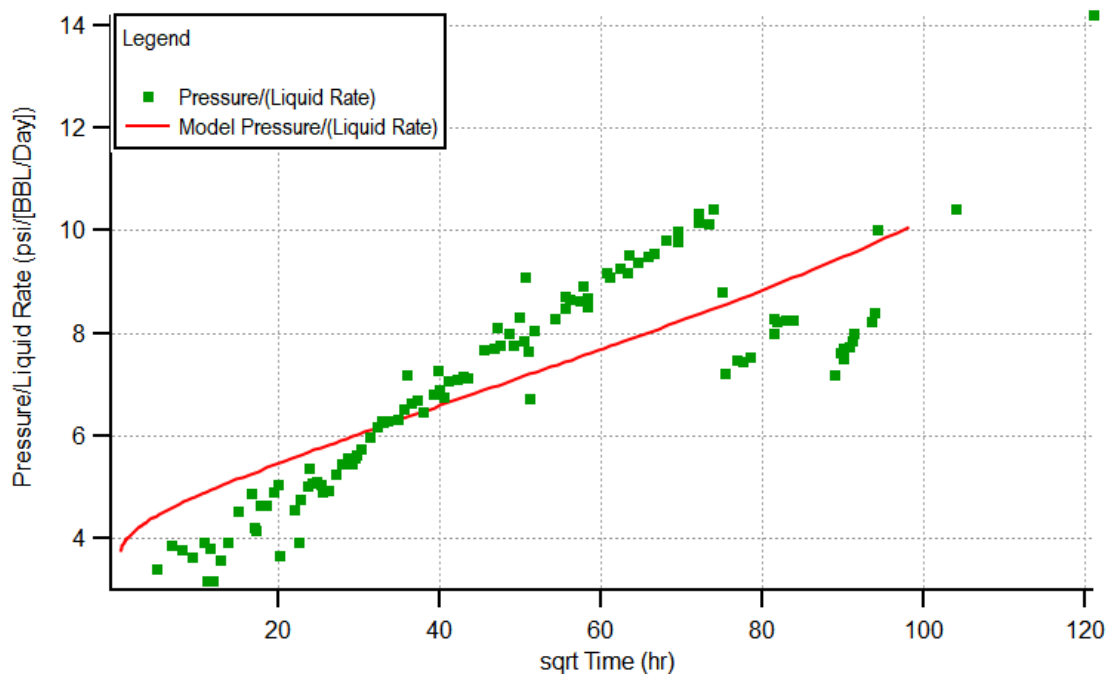


Figure 3.3 — Well 3 Linear Flow Plot (with RTA model imposed)

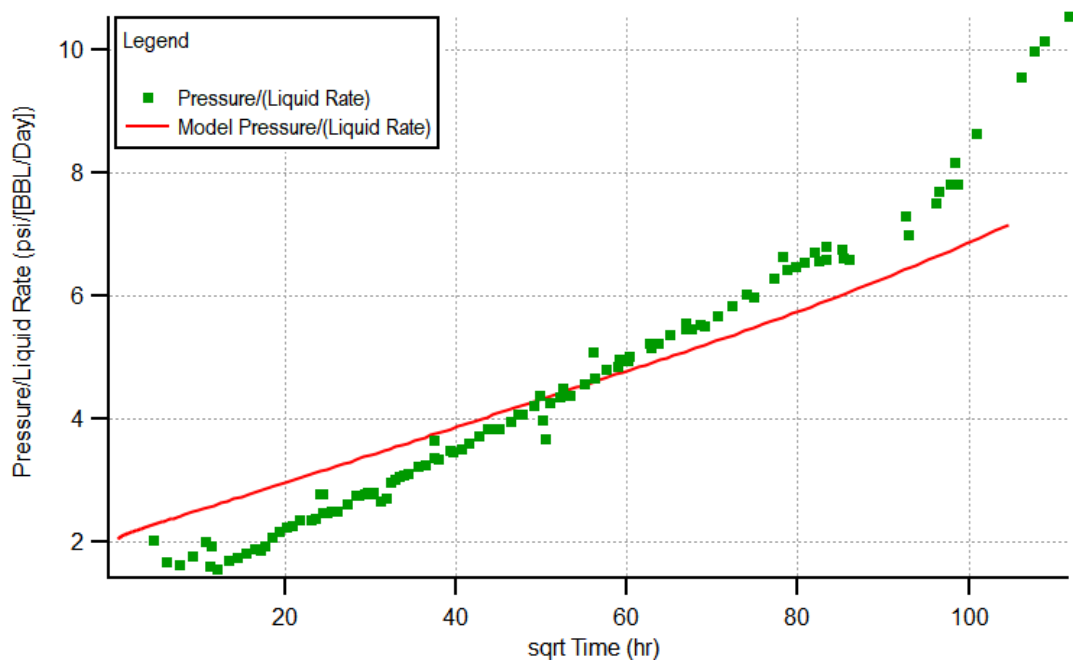


Figure 3.4 — Well 4 Linear Flow Plot (with RTA model imposed)

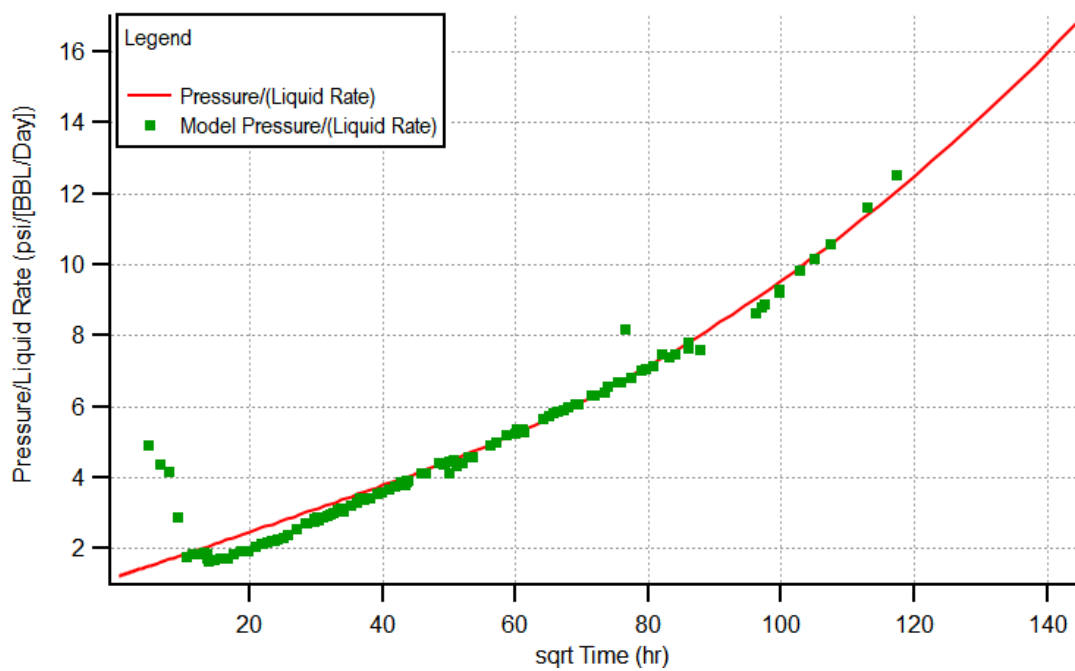


Figure 3.5 — Well 5 Linear Flow Plot (with RTA model imposed)

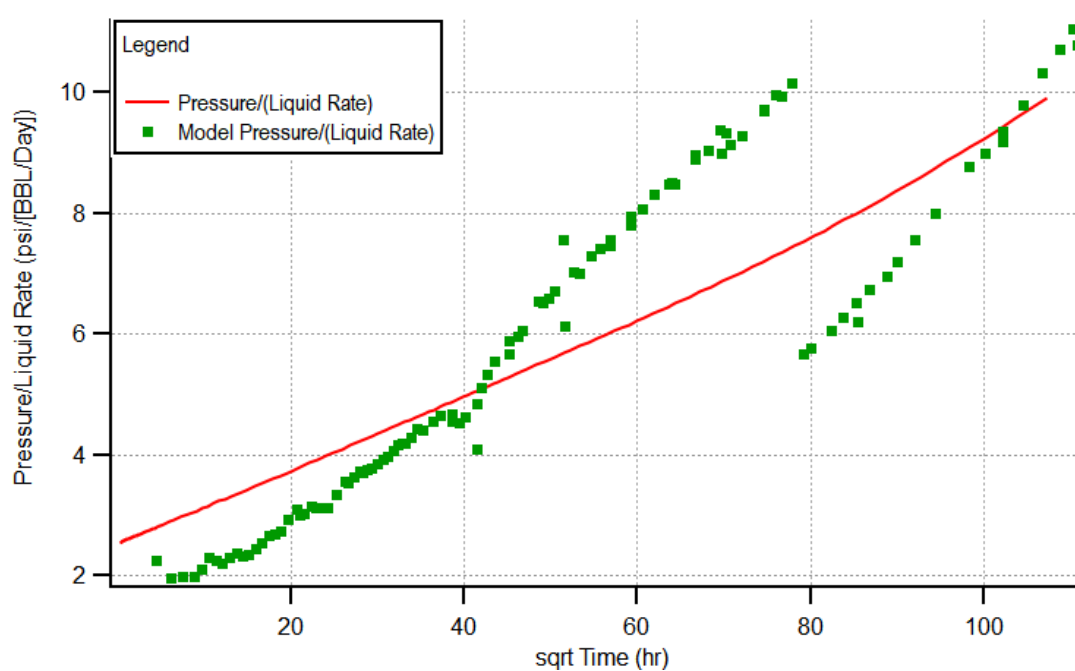


Figure 3.6 — Well 6 Linear Flow Plot (with RTA model imposed)

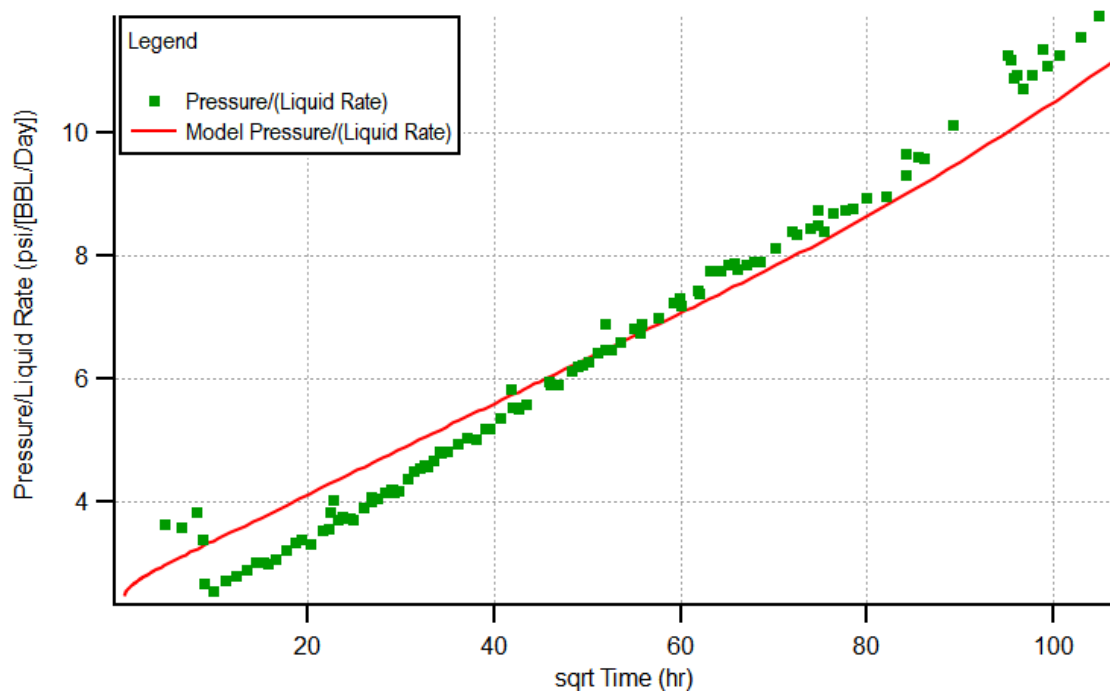


Figure 3.7 — Well 7 Linear Flow Plot (with RTA model imposed)

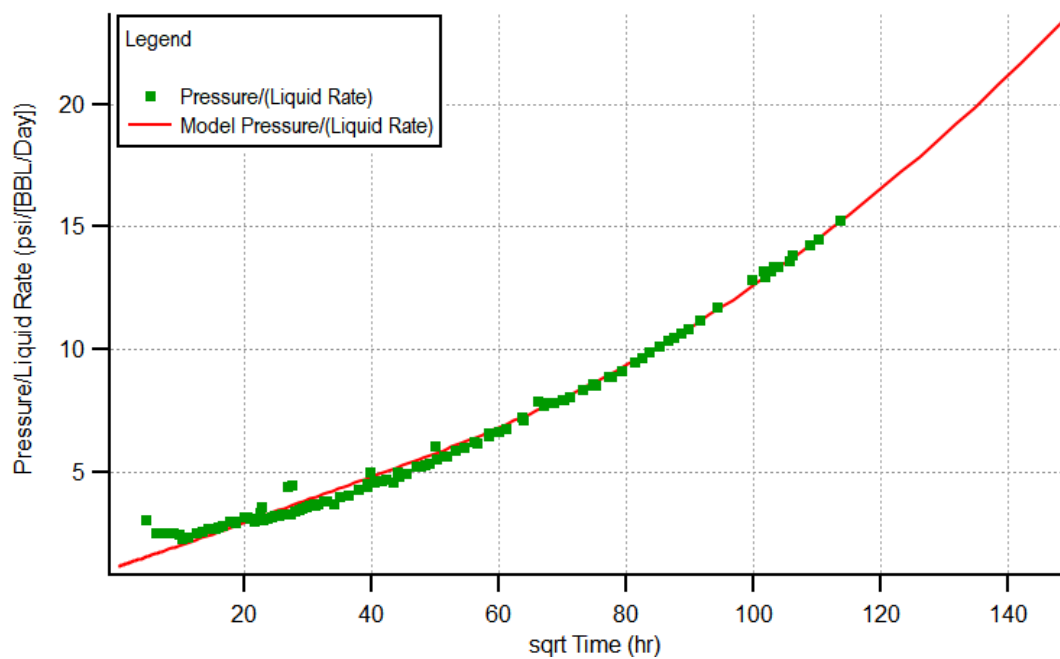


Figure 3.8 — Well 8 Linear Flow Plot (with RTA model imposed)

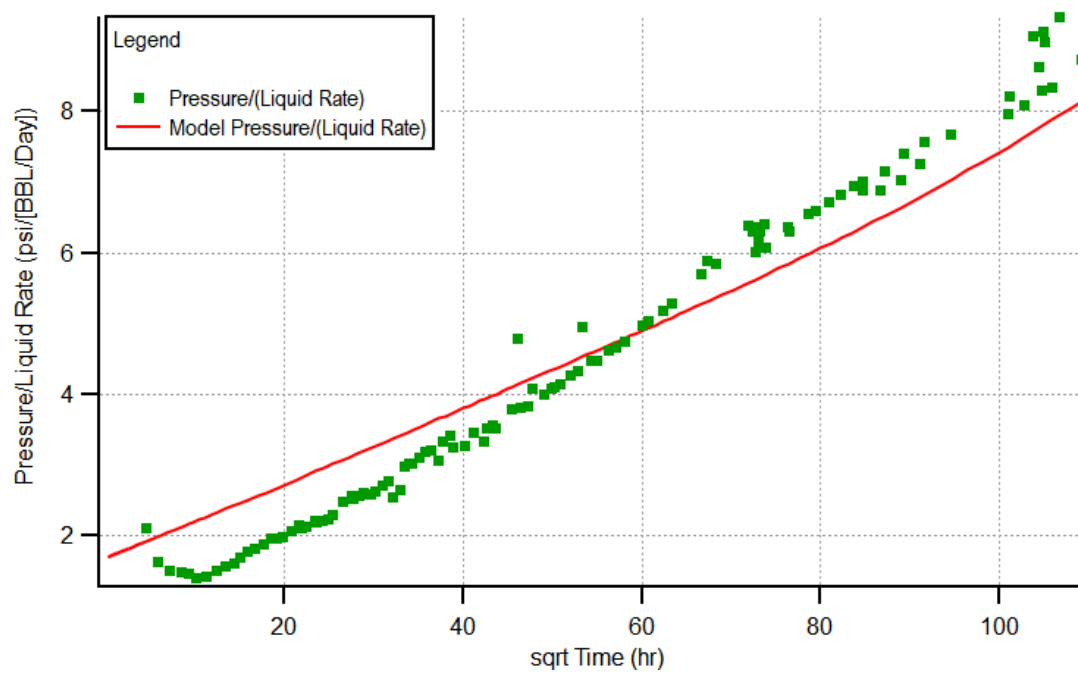


Figure 3.9 — Well 9 Linear Flow Plot (with RTA model imposed)

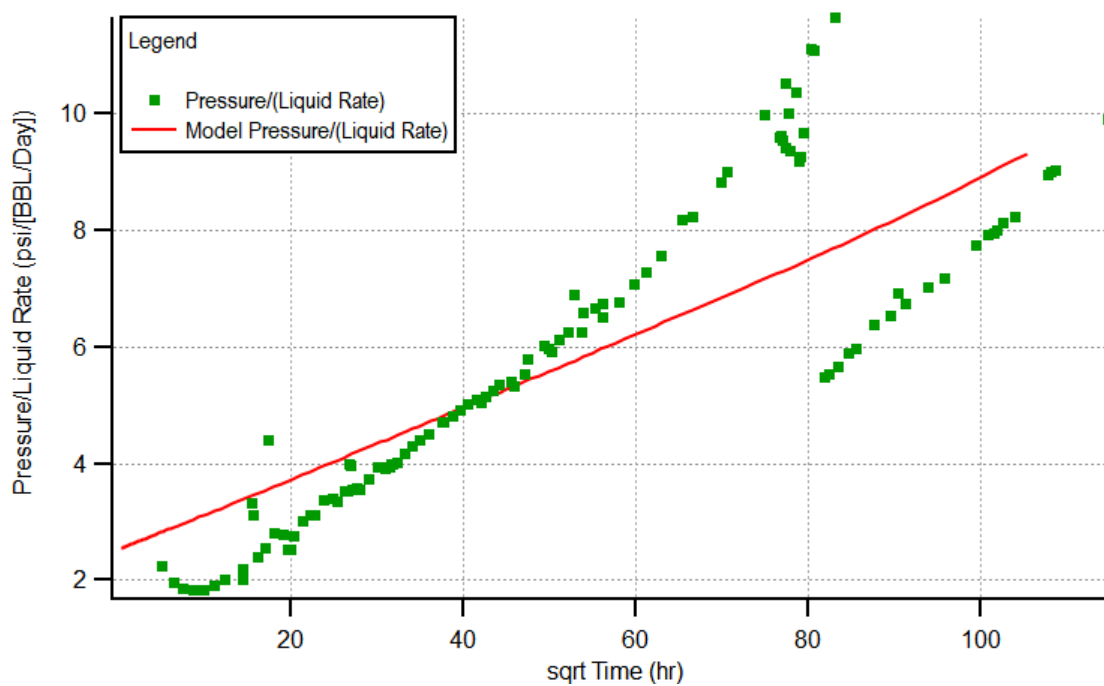


Figure 3.10 — Well 10 Linear Flow Plot (with RTA model imposed)

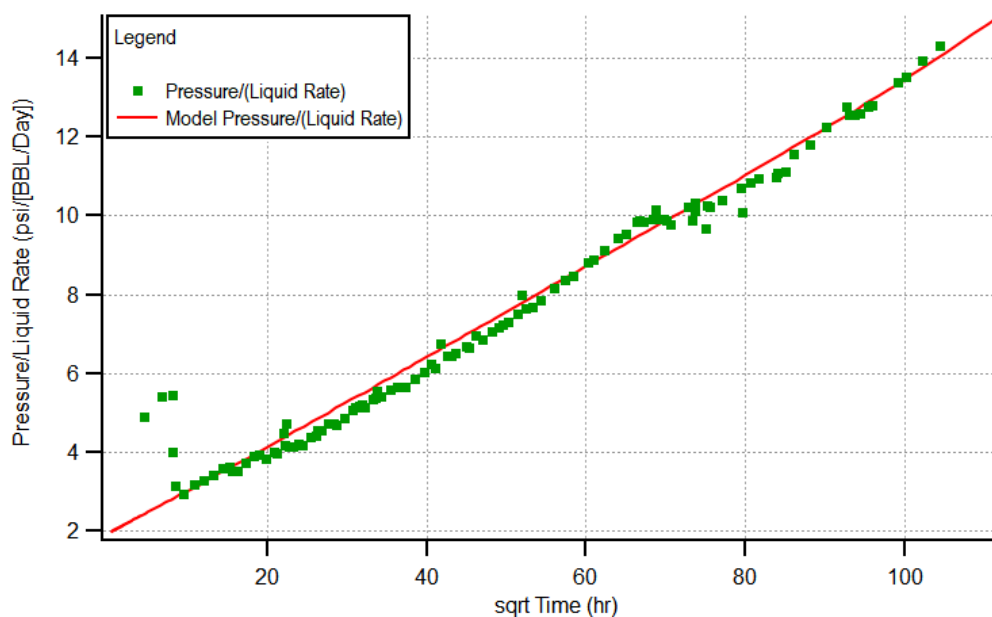


Figure 3.11— Well 11 Linear Flow Plot (with RTA model imposed)

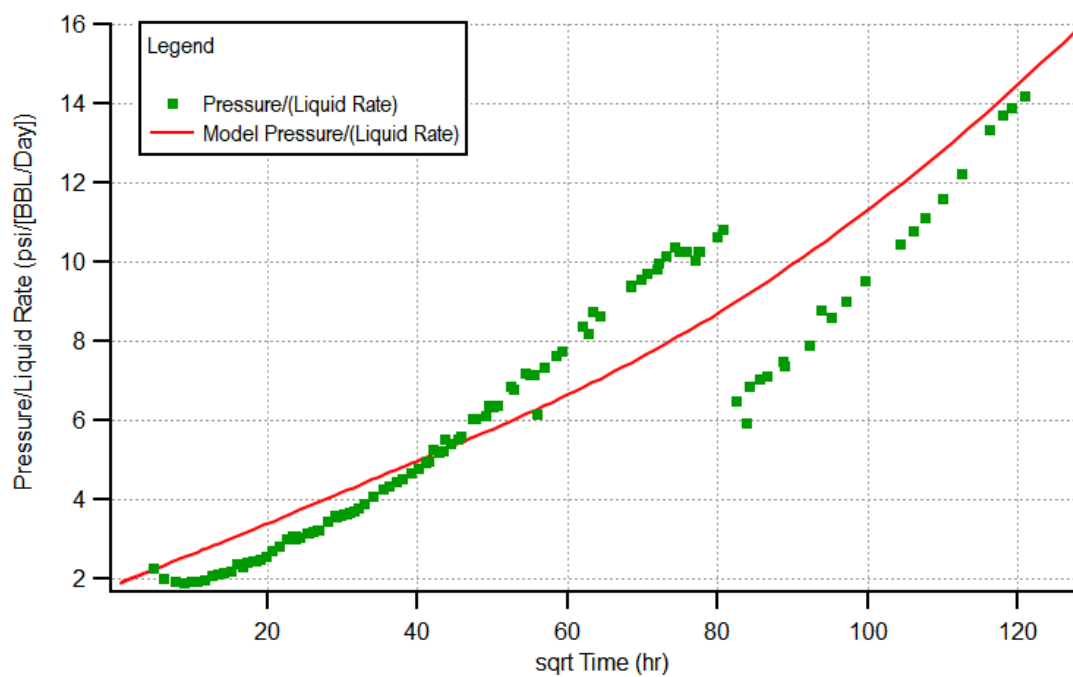


Figure 3.12— Well 12 Linear Flow Plot (with RTA model imposed)

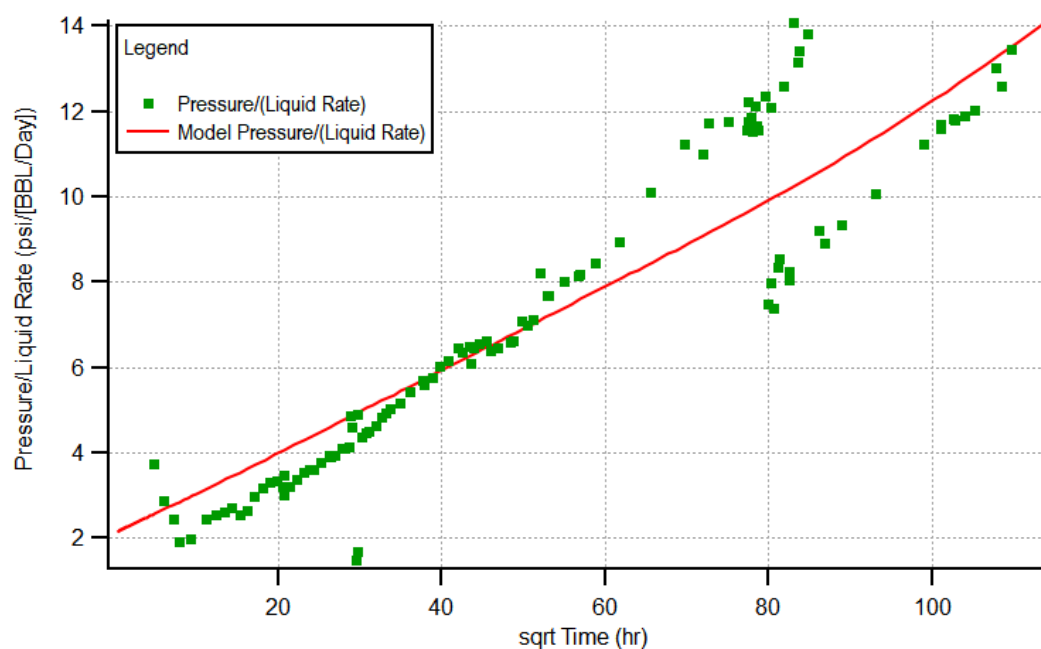


Figure 3.13— Well 13 Linear Flow Plot (with RTA model imposed)

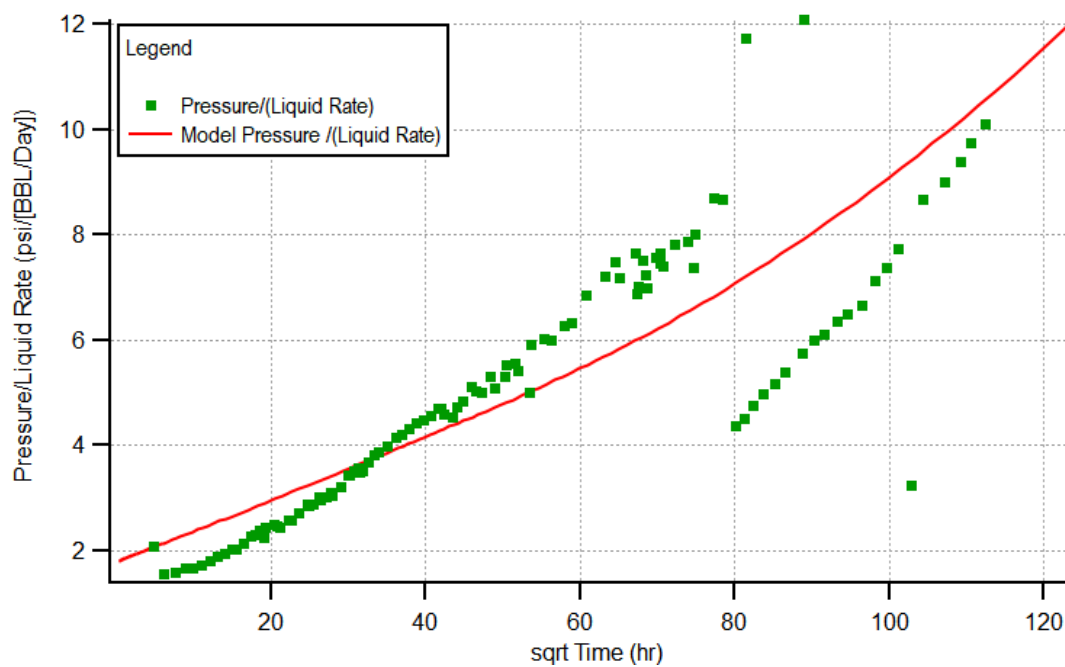


Figure 3.14— Well 14 Linear Flow Plot (with RTA model imposed)

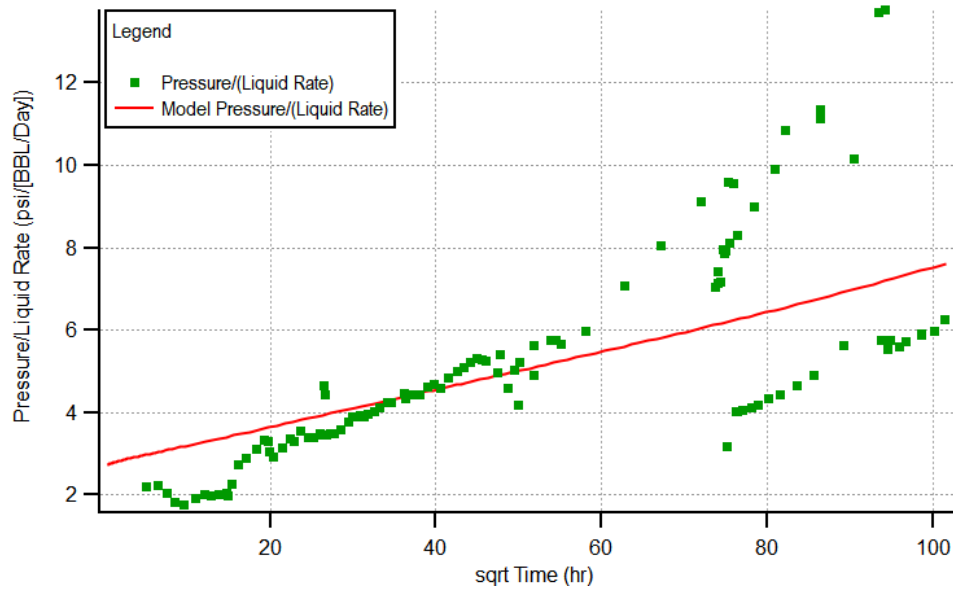


Figure 3.15— Well 15 Linear Flow Plot (with RTA model imposed)

3.2 Discussion of Results

The RTA "Linear Flow" plots are presented in **Figs. 3.1-3.15** (data are represented by the green symbols (squares) and the model trends are given by the red trendlines). This format of these plots (*i.e.*, the reciprocal productivity index versus the square root of production time) is used to try to illustrate the "linear flow" dominated data (which would appear as a straight-line on this plot). One can observe that there are several cases where the data-model matches are not as strong as would be preferred. Well 5 (**Fig. 3.5**), Well 8 (**Fig. 3.8**), and Well 11 (**Fig. 3.11**) show excellent data-model matches, and one can interpret that the concept of "linear flow" is clearly validated for these cases.

As comment, most of the "mismatch" cases appear to have operational issues (*i.e.*, intended and/or unintended shut-ins), but this is somewhat speculative, our stated goal is to analyze all cases so we considered the "best fit" as well as the mismatch cases in our analysis and interpretation efforts.

Based on this work, we believe that the Lower Wolfcamp A wells will generally reach the end of linear flow faster than the Upper Wolfcamp A and the Upper Wolfcamp B wells. In addition, the Upper Wolfcamp A wells appear to achieve the end of linear flow much slower compared to the Lower Wolfcamp B wells, suggesting additional drawdown opportunities. These observations are somewhat qualitative; but are also correlative with the known well completion information that were reviewed as part of this work.

CHAPTER 4

PRESSURE TRANSIENT ANALYSIS

4.1 Orientation to Pressure Transient Analysis

In general, pressure transient analysis work utilizes high frequency/high resolution bottomhole pressure data (frequency on the order of seconds or minutes and resolution on the order of 0.01 psi) to develop appropriate insights for buildup or drawdown. High frequency/high resolution data often provide evidence of reservoir features or flow regimes that might not have been captured in (daily) production rate and pressure data.

However, for applications in unconventional reservoirs it is relatively rare to have access to high frequency/high resolution bottomhole pressure data — but in this work, we do have such data for seven out of the fifteen wells selected for detailed study.

It is also critical to recognize that with so much resolution, these data will reflect operational events, well interference, well operations, etc. with a magnified emphasis. In short, we may not observe the features we see to witness because of operations and other factors. This is mentioned for orientation as most of our pressure buildup test data are (apparently) severely affected by operations activities.

In this work, the commercial PTA program "Sapphire" (Kappa Engineering) was used and although the data are severely affected by operational aspects (particularly at early times), we made an effort to analyze all wells. The operator believes that these severely affected data are due to wellbore loading during the pressure buildup test (this is a common malady in PTA for unconventional reservoirs)

In **Table 4.1**, we present the "limiting values" of the various parameters we are seeking to estimated (these parameters are provided for reference).

Table 4.1 — Maximum Values Possible for Various Parameters

Parameter	Maximum Value Possible
Number of Fractures	897
Fracture Half length (ft)	300
Fracture Conductivity (md-ft)	1000
Permeability (md)	9.E-06

In **Table 4.2**, we provide the PTA results and compare these results to those results for the same wells for the same wells.

Table 4.2 — Results comparisons — PTA and RTA

Well	Landing Zone	PTA					RTA				
		k	kh	h	Pi	s	k	kh	h	Pi	s
2	Middle Wolfcamp	0.032	6.35	198.44	3500	0.032	6.36E-6	1.91E-3	300.31	5949	0.0000513
4	Upper Wolfcamp (Top)	0.019	3.9	205.26	3300	0	4.94E-6	1.48E-3	292.94	5144	2.20E-05
5	Middle Wolfcamp	0.014	2.86	204.29	4000	0	7.65E-6	2.30E-3	299.06	5949	0.0000287
7	Upper Wolfcamp (Bottom)	0.114	22.71	199.21	2800	0	4.61E-6	1.27E-3	245.06	5705	0.0000224
8	Middle Wolfcamp	0.017	5.11	300.59	3800	4.6E-4	7.82E-6	2.36E-3	238.62	5949	0.0000285
9	Upper Wolfcamp (Top)	0.015	4.56	304.00	3200	0	5.14E-6	1.54E-3	262.14	5144	0.0000193
11	Upper Wolfcamp (Bottom)	4.11E-3	1.23	299.00	2800	0	4.58E-6	1.37E-3	250	5705	0.0000199

We immediately note that the kh -values estimated using the PTA methodology are much higher than the kh -values assumed for the RTA methodology. The log-log analysis/interpretation plots are provided in **Figs. 4.1-4.7**, where we again noted that the matches of the pressure drop and pressure drop derivative functions are qualitative at best.

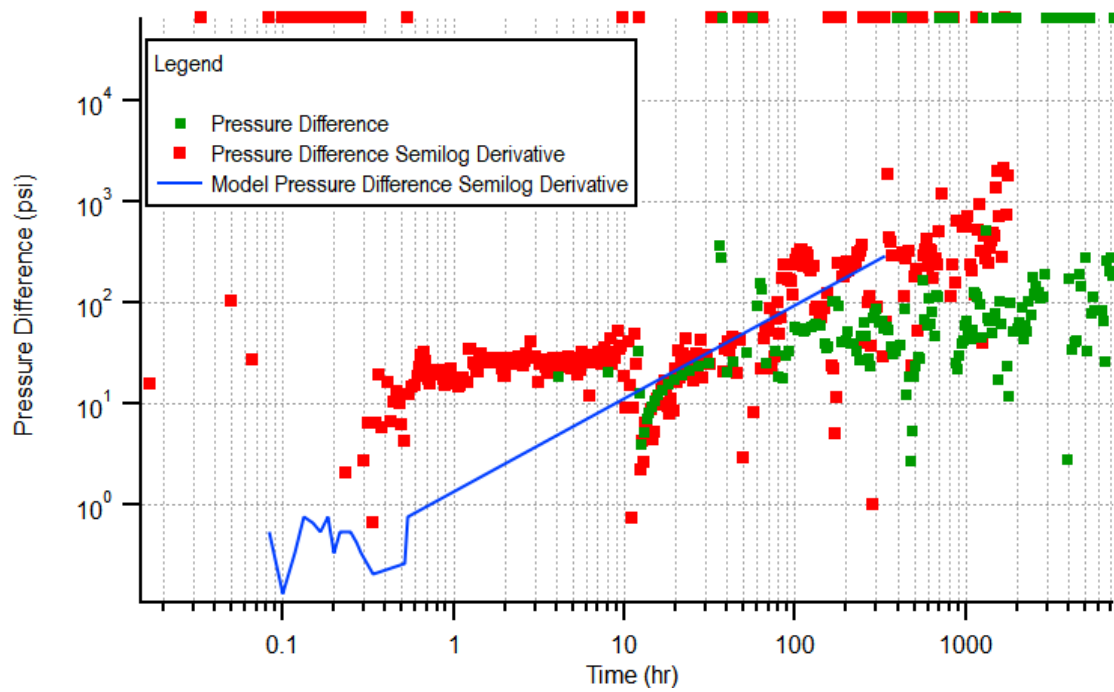


Figure 4.1 — Well 2 Log-Log Plot (with PTA model imposed).

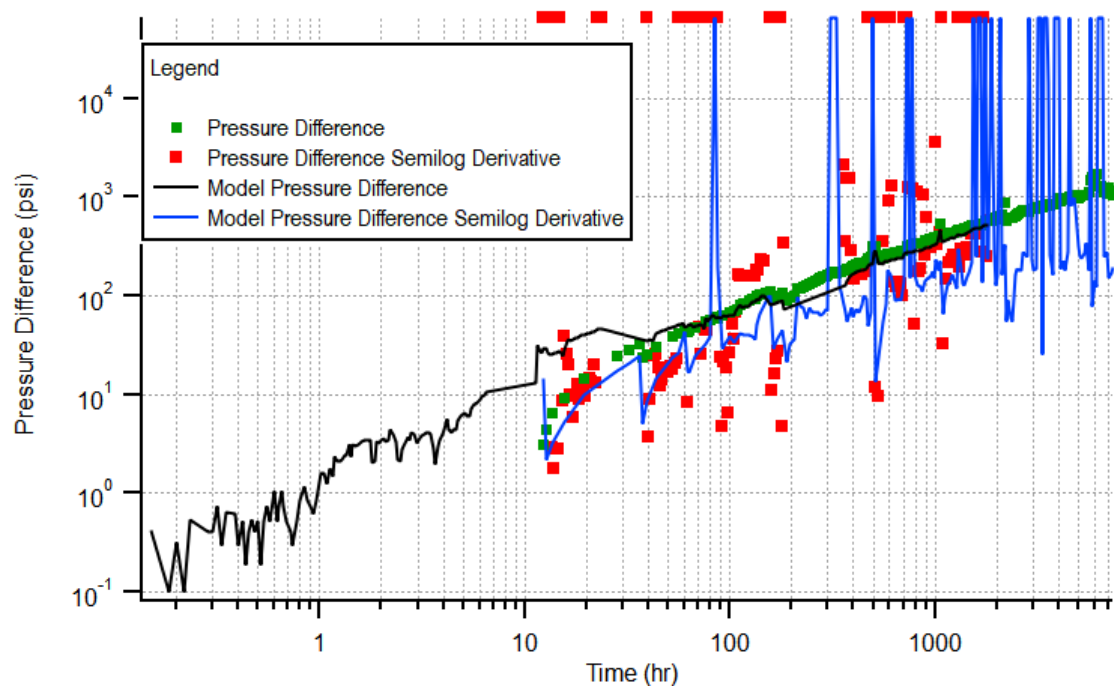


Figure 4.2 — Well 4 Log-Log Plot (with PTA model imposed).

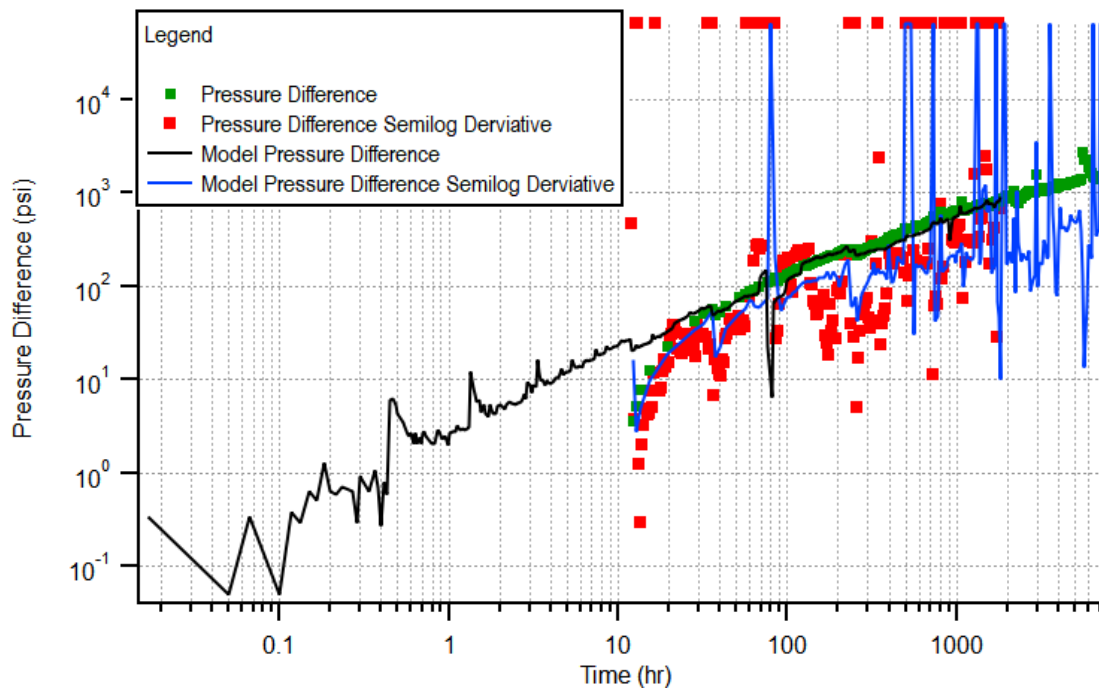


Figure 4.3 — Well 5 Log-Log Plot (with PTA model imposed).

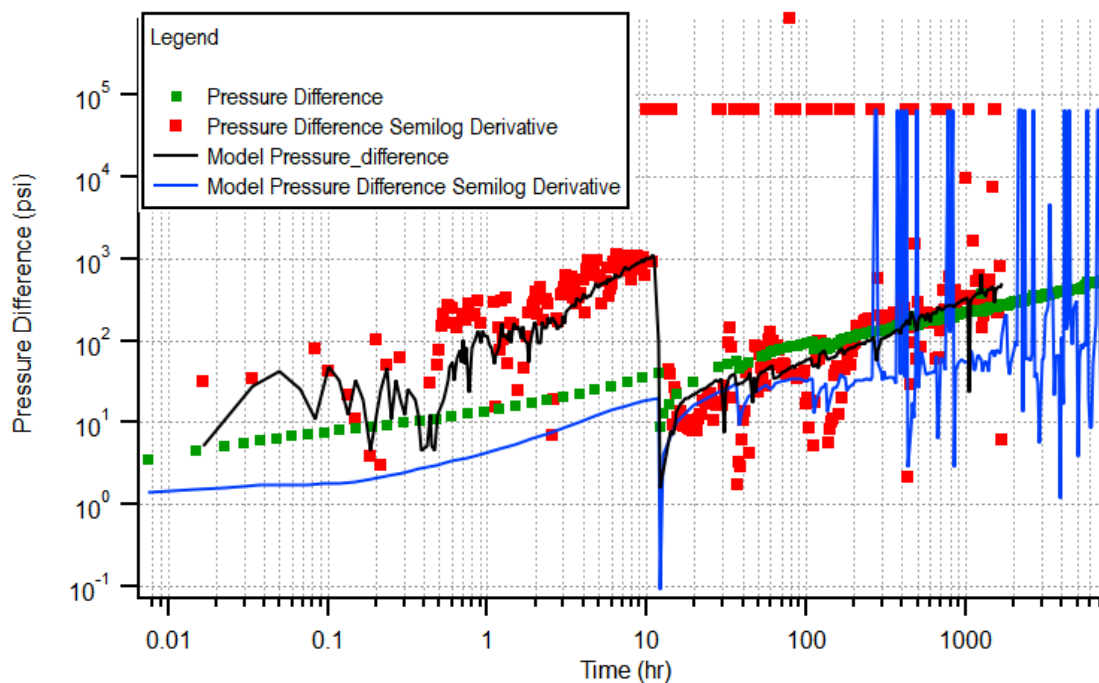


Figure 4.4 — Well 7 Log-Log Plot (with PTA model imposed).

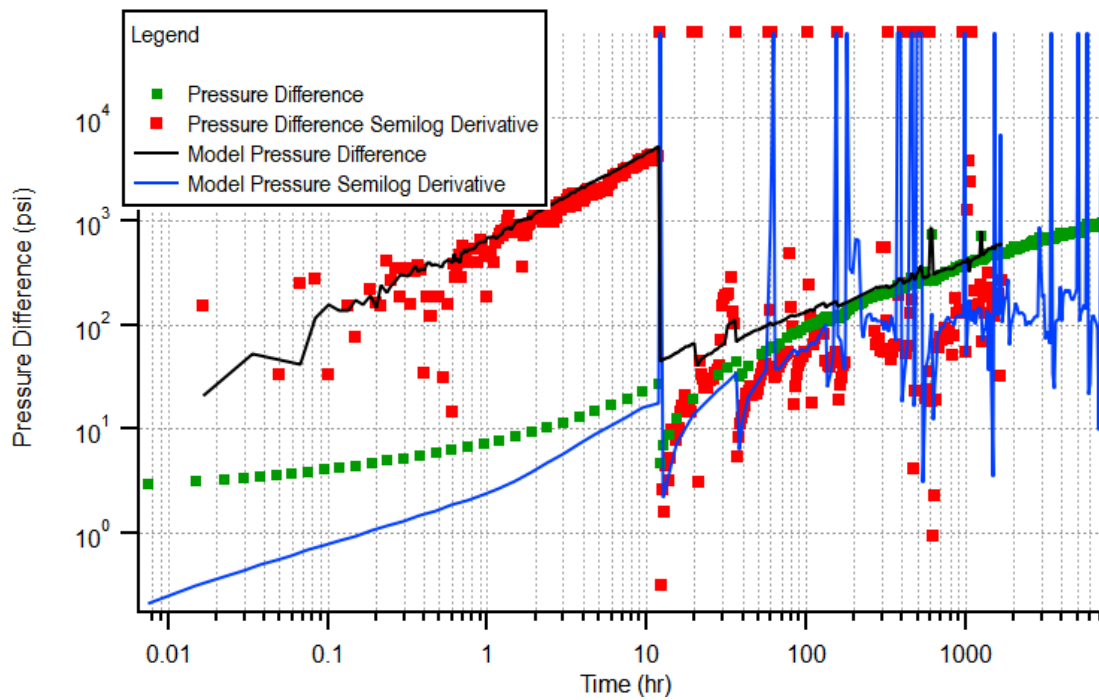


Figure 4.5 — Well 8 Log-Log Plot (with PTA model imposed).

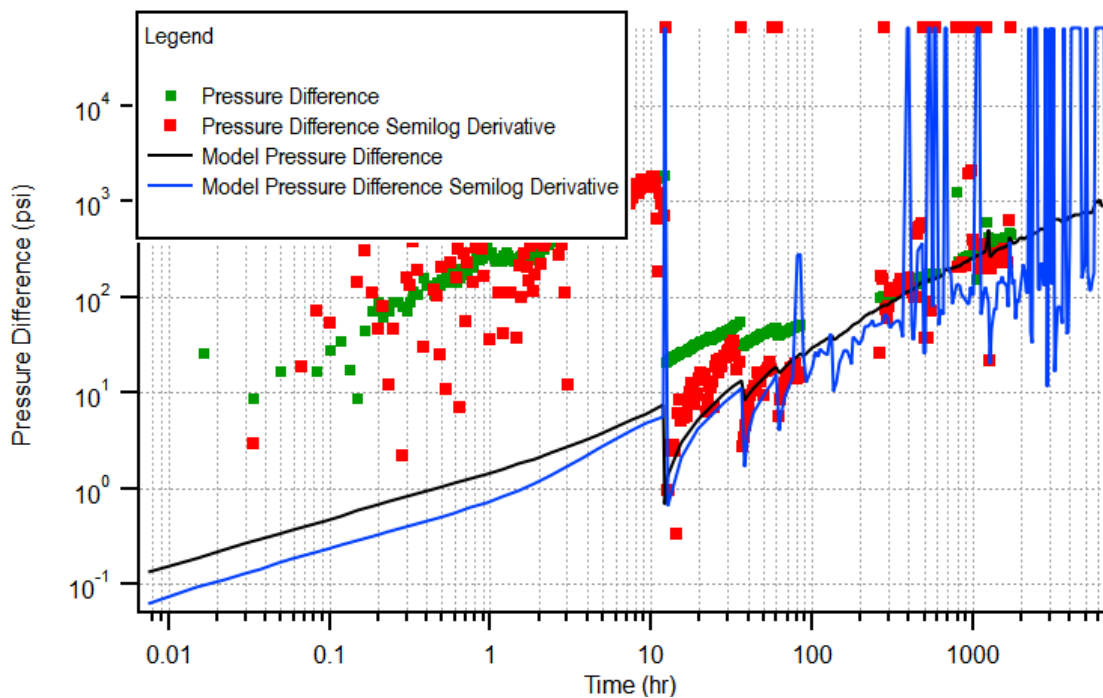


Figure 4.6 — Well 9 Log-Log Plot (with PTA model imposed).

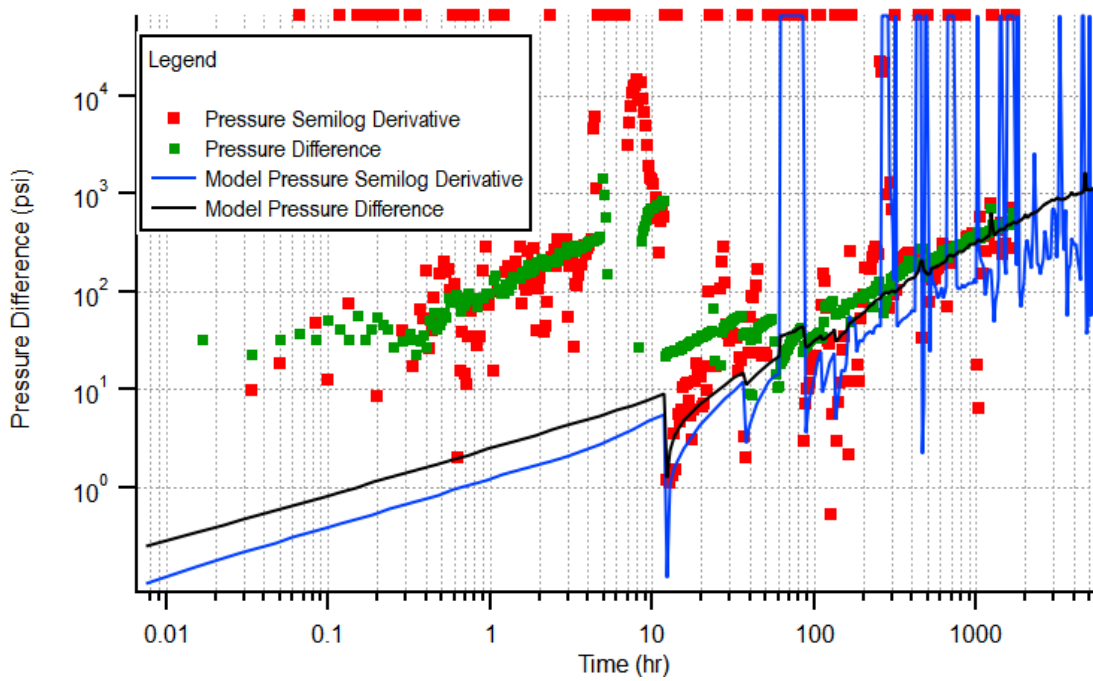


Figure 4.7 — Well 11 Log-Log Plot (with PTA model imposed).

4.2 Discussion of Results

First and foremost, although the data for these analyses were obtained by high frequency/high resolution bottomhole pressure gauges, the data reviewed for these pressure buildup cases have an enormous volume of noise (and operational effects in some cases). We believe that the generally poor behavior of the pressure data for these cases is due to wellbore load-up during the flowback and early time production data.

As comment, we would recommend that future efforts focus on specifically designed shut-in cases where the wells are conditioned (*i.e.*, maintained at as a constant rate as possible for several days prior to shut-in), this will lead to much better data trends, interpretations, and analyses.

CHAPTER 5

NUMERICAL MODELING

5.1 Orientation to Numerical Modeling

To develop the numerical models, the commercial software "CMG" (Computer Modeling Group) was used. Each wellbore model is a simple horizontal well model of 10,000 ft in length (i-direction) with imported pressure and production data for the history match. **Table 5.1** displays the general reservoir properties for the Wolfcamp formations.

Table 5.1 — General Reservoir Properties

Property	Unit	Value
Porosity	(fraction)	0.06
Thickness	ft	300-400
Water Saturation	(fraction)	0.5-0.7
Matrix Permeability	nd	800

Modeling Assumptions:

Creating the Grid

When creating the grid, the reservoir domain was discretized into 540 gridblocks in the i-direction and 100 gridblocks in the j-direction. There are varying levels in the i-direction to reflect fractures and 10 ft. in the j-direction. Finally, there are 10 layers in the k-direction (this is the "z-direction"), with each layer at 50 feet for the Wolfcamp B model and 25 ft for the Wolfcamp A model. The tops of the grid reflect the tops of each formation. A single porosity model is assumed in order to develop this model as there is no evidence of contributions from natural fractures. **Figs 5.1 and 5.2** shows the grid with all of the wells in the Wolfcamp A and Wolfcamp B formations, with configurations reflecting the gun barrel view.

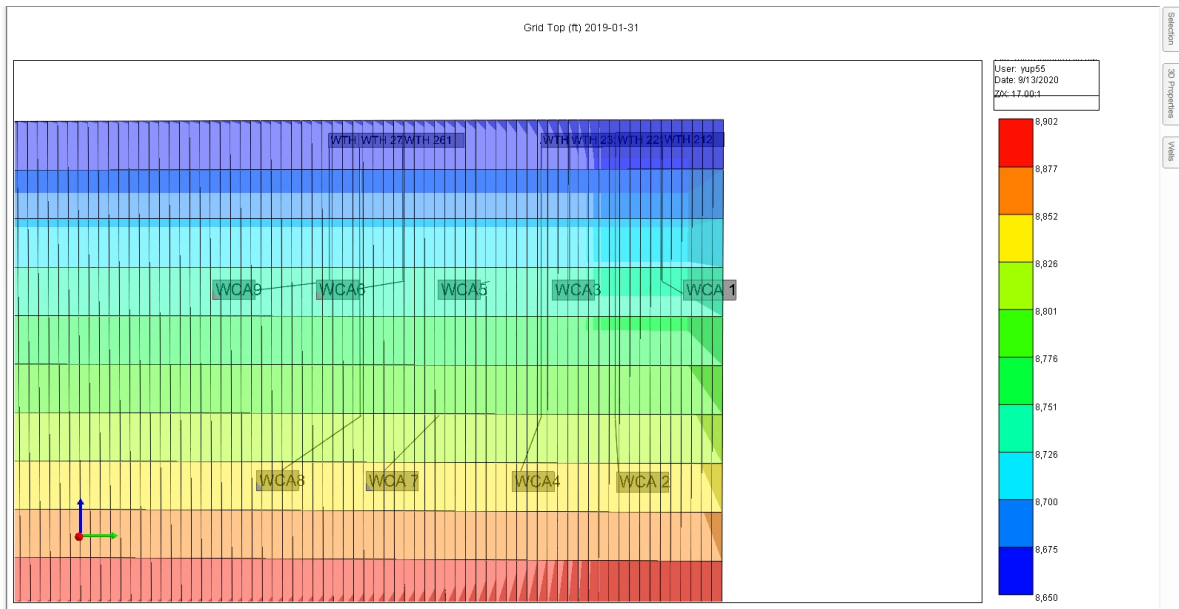


Figure 5.1 — Configuration of Upper and Lower Wolfcamp A Wells.

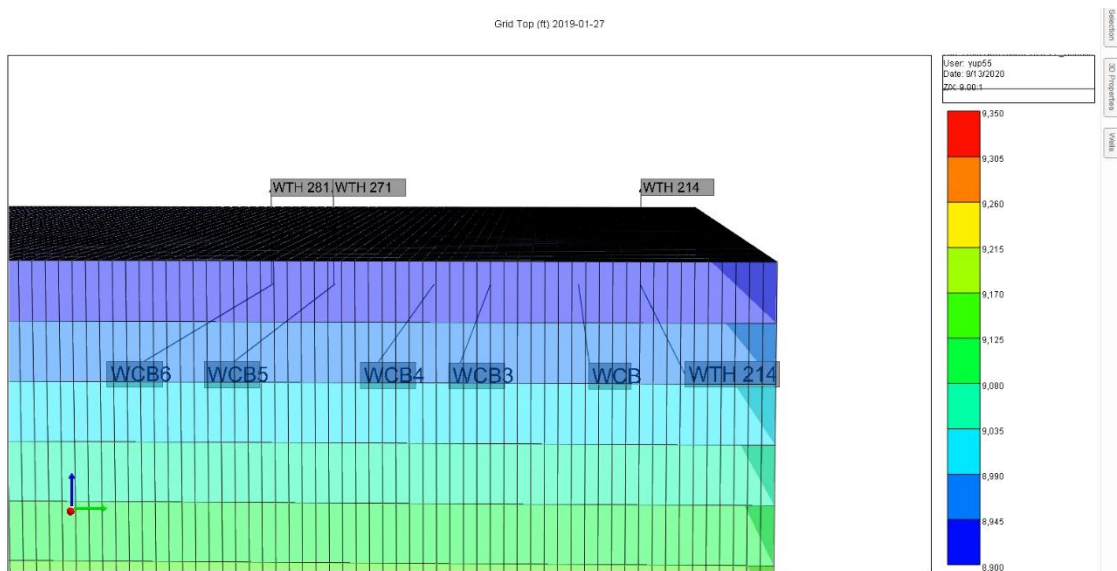


Figure 5.2 — Configuration of Wolfcamp B Wells.

The Stimulated Reservoir Volume (SRV) is defined as a single grid block from each side of the wellbore with an enhanced permeability zone throughout the wellbore. Additionally, fractures were created with an assigned fracture permeability, assuming a 150 ft stage spacing and with each stage having a single fracture.

To conserve computation times for the Wolfcamp A cases, single-well models were later created for each well, as different sets of relative permeability curves were required for each well. A portion of the model was created for Wolfcamp A, where approximately 1/10th of the well is modeled.

Well Creation and Constraints

For each well, a model is defined as a straight wellbore of 10,000 ft in the i-direction of the grid. There are geometric perforations in each block to reflect a perforated length of 10,000 length. When defining well constraints, the minimum flowing bottomhole pressure is constrained to the last flowing bottomhole pressure datum from the field history. History matches were based on these bottomhole pressure control constraints.

Sensitivity Analyses

To run the sensitivity analyses and history matches, the commercial reservoir simulator CMG-IMEX was used. The following scenarios were run for each well in the sensitivity analyses work, depending on whether or not the well had already reached its minimum flowing bottomhole pressure constraint from the original field history:

- 1000 psi (conservative)
- 800 psi (moderate)
- 500 psi (aggressive)

To expedite modelling the well performance to yield a 30-year EUR, a sector model for each well was used to forecast production rates. This was required for the Wolfcamp A model because of extensive computation time to run 9 wells in one model (and even for just a single well being produced to 30 years). This means that a group of grid blocks used for the well model were used to observe the production trends and will then be scaled up to the entire wellbore. Bottomhole pressure declines will depend on the parameters used for each well on their respective history

matches. However, the scenarios described above will represent the minimum and the continuous flowing bottomhole pressure once the well reaches that value during the forecast.

5.2 Numerical Modeling Cases

Case 1: Primary-Infill Scenarios

Wolfcamp A

Well 1 is an infill well to an offset competitor well that has been producing five months prior to the production of Well 1. Because this is an infill well, asymmetrical fractures and pressure depletion could contribute to lower initial rates. **Table 5.2** shows the oil EUR for the different drawdown scenarios used in this case.

Table 5.2 — Post History Match Drawdown Strategies for Primary-Infill Scenario

Case	Minimum Flowing Bottomhole Pressure (psia)	Oil EUR (MBO)
Base	2300	668
Conservative	1000	177
Moderate	800	1356
Aggressive	500	160

The moderate drawdown case yields the highest EUR compared to the conservative and aggressive cases. It is important to note that since these are single porosity models, EUR values tend to be lower because there are no contributions from natural fractures. The moderate case may have matrix contributions during the later portion of the well life. For the moderate case, further investigation is needed regarding possible numerical instabilities which may have occurred during the later portion of the well life.

Wolfcamp B

Well 2 is the case of a Wolfcamp B primary-infill case. Well 2 is also an infill well to an offset competitor well that has also been producing five months prior to the production of Well 2. Similar to the Wolfcamp A infill case (Well 1), asymmetrical fractures and pressure depletion could contribute to lower initial rates. **Table 5.3** shows the oil EUR for the different drawdown scenarios used in this case:

Table 5.3 — Post-History Match Drawdown Strategies for Primary-Infill Well Scenario

Case	Minimum Flowing Bottomhole Pressure (psia)	Oil EUR (MBO)
Base	2300	670
Conservative	1000	1680
Moderate	800	1823
Aggressive	500	1960

In this special case, the drawdown strategy significantly improved the oil EUR-values. The aggressive case ($p_{wf,min} = 500$ psia) led to be best recovery for this case (1960 MBO).

Case 2: Co-Developed Cases

Wolfcamp A

Well 9 is co-developed Wolfcamp A case — Well 9 is located between other wells, where all wells were put on production at the same time.

Table 5.4 presents the oil EUR for the different drawdown scenarios used in this case:

Table 5.4 — Post History Match Drawdown Strategy for Co-Developed Cases

Case	Minimum Flowing Bottomhole Pressure (psia)	Oil EUR (MBO)
Base	2300	133
Conservative	1000	681
Moderate	800	1346
Aggressive	500	681

In this scenario, the moderate drawdown case yields the highest oil EUR-value. Similar to the previous Wolfcamp A case, more investigation is needed on potential model instabilities that may have limited production in the case of the aggressive pressure drawdown case.

Wolfcamp B

Well 8 is the co-developed Wolfcamp B case and is located between other wells, where all wells were put on production at the same time. **Table 5.5** presents the oil EUR for the different drawdown scenarios used in this case:

Table 5.5 — Post History Match Drawdown Strategy for Co-Developed Cases

Case	Minimum Flowing Bottomhole Pressure (psia)	Oil EUR (MBO)
Base	2300	634
Conservative	1000	1624
Moderate	800	1759
Aggressive	500	1887

Similar to the primary-infill case, the aggressive pressure drawdown case yielded the highest EUR-value of 1887 MBO, where this performance suggests that the minimum drawdown pressure can make a significant difference in the well performance.

Case 3: Well Close to a Fracture Barrier (Lower Wolfcamp A):

Well 3 is used for the case of a well close to a fracture barrier case, Well 3 is a co-developed and is landed near a fracture barrier. **Table 5.6** presents the oil EUR for the different drawdown scenarios used in this case:

Table 5.6 — Post History Match Drawdown Strategies for Well Near Fracture Barrier

Case	Minimum Flowing Bottomhole Pressure (psia)	Oil EUR (MBO)
Base	2300	281
Conservative	1000	441
Moderate	800	637
Aggressive	500	471

In this case the moderate pressure drawdown case yields the highest EUR. To reiterate our perception from the other Wolfcamp A cases, this observation may be due to matrix contributions during the later portion of the well life. An interesting anomaly is that the aggressive pressure drawdown case yields higher EUR-values than the conservative case. As with other cases, we suspect that there may be numerical instability issues in some of the cases. This is an opportunity for further investigation.

Drawdown Management Strategies: Pre-History Matching:

Prior to performing matching in our workflow, synthetic flowing bottomhole pressure profiles were developed using Crespo et al's definitions of drawdown management strategies:

- Conservative- .5-1 psi/hr (.75 psi/hr used)
- Moderate- 1-2.5 psi/hr (1.75 psi/hr used)
- Aggressive- 2.5-5 psi/hr (3.75 psi/hr used)
- Very Aggressive- 5-10 psi/hr (7.5 psi/hr used)

Synthetic Pressure Profiles

In this section we consider the cumulative production behavior of different cases of wells using prescribed minimum flowing bottomhole flowing pressures. The conservative, aggressive, very aggressive and moderate cases are presented for a Wolfcamp B well in **Fig 5.3**.

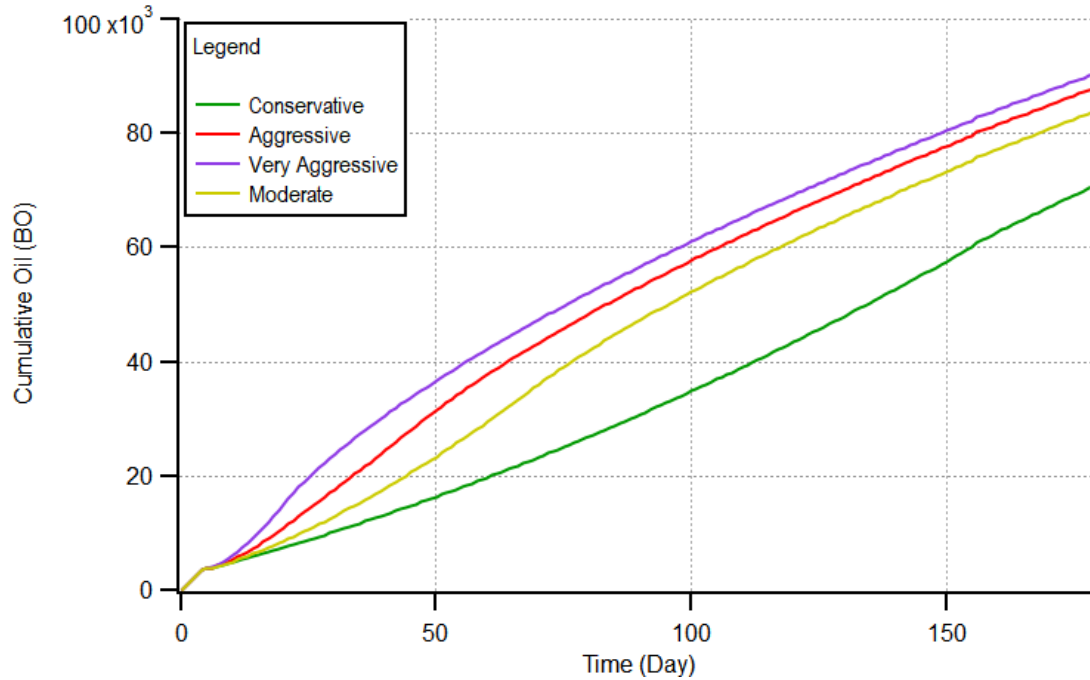


Figure 5.3 — Cumulative Oil Production Results for the Wolfcamp B Wells.

From **Fig. 5.3** we note that the conservative drawdown strategy yields the lowest cumulative production in the first six months, whereas the very aggressive scenario yields the highest cumulative production. There is a marginal difference between the aggressive and very aggressive scenarios for this case. This work shows that it is the minimum bottomhole pressure that makes the most difference in recoveries, while the beginning drawdown strategy provides only a marginal uplift in recovery. The remaining scenarios for Wolfcamp A and Wolfcamp B also reflected this pattern where the conservative drawdown strategy in early time provided the least recovery and where the very aggressive pressure drawdown case provided the highest recovery.

5.3 Discussion of Results

Relative Permeability

To state this explicitly, we believe that the role of relative permeability is source of the largest uncertainty in the reservoir modeling portion of the workflow. Our primary goal is to investigate drawdown strategies in a multi-well scenario — however; each well has different set of relative permeability curves, and the limitation for a multi-well scenario is when applying the same set of curves for all of the wells, less than optimal matches will be obtained.

As an example, the Upper Wolfcamp A and Lower Wolfcamp A cases had to be modeled separately for this reason. Additionally, some wells had to be modeled separately as single well cases because the relative permeability curves are unique to the given well. Another complication for relative permeability is matching oil production performance in the early time period, especially for the Upper Wolfcamp A wells. It is imperative to measure relative permeability curves for all three phases (Chhatre et al 2019). We also note that the relative permeability matches for this work were obtained using the commercial software "CMOST".

Fracture Geometry

In reservoir simulation, the fracture geometry is another uncertainty. Fractures in this work were assumed to be symmetrical, with the pressure depletion dependent on the different fracture permeabilities assigned to a given well. In addition, because natural fracture density is uncertain in our proposed landing targets, a single porosity model was used to simplify the model.

Pressure Declines

Calculated flowing bottomhole pressures used in this work are based on either the depth of the gauge or on the tubing pressure values. For some wells, the bottomhole pressure gauges stopped working, and the tubing pressure had to be used to estimate the flowing bottomhole pressure.

There are several instances where the pressure and rate profiles do not match well (e.g., cases where there are missing pressure data). We realize that such discrepancies in the measured data can lead to poor/less-than-optimal history matches. For the purposes of this work, we assume that a given match is acceptable for forecasting if the latter portion of the oil production history is matched.

Water Production

Water trends were not the focus of this study, and the mediocre to poor matches obtained were due to the uncertainty of the relative permeability curves. There continues to be an industry study in the Midland Basin of the drivers of relatively high water production. A balance must be achieved between matching water production at early time or matching the oil production at early time. Since the results are focused on optimizing oil EUR, matching oil production, and using flowing bottomhole pressure controls took priority.

PVT and GOR

Cases which exhibited high gas rates were difficult to match because of the low bubblepoint pressures of the oils in the Midland Basin. For this work, **Fig 5.4** shows the GOR profiles obtained using various drawdown strategies.

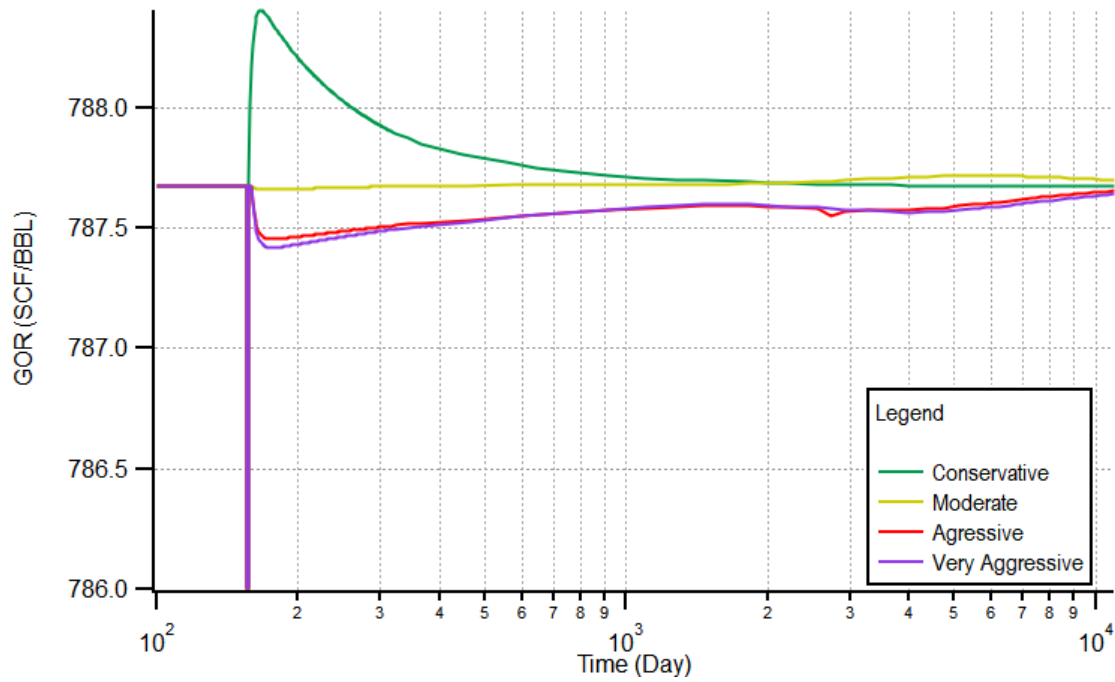


Figure 5.4 — Gas-Oil-Ratio (GOR) Trends from Numerical Modelling Cases.

In **Fig. 5.4** we can conclude that no matter the pressure drawdown strategy, the effect on the GOR trends for the cases is at best minor, and more likely negligible. However, in practice, the influence of the pressure drawdown strategy can be significant to severe. We believe that the relatively low GOR nature of these fluids along with the nature of the specified relative permeability curves has led to these essentially minimal influences on the GOR regardless of the production strategy.

CHAPTER 6

FRACTURE MODELING

6.1 Orientation to Fracture Modeling

In this chapter we address specifically the modelling of the hydraulic fractures. We have elected to use the GOHFER software suite (this is an industry-standard package). As process, deviation surveys, LAS files, and hydraulic fracture treatment data for the selected wells were imported into the GOHFER-3D package.

The wells of interest were those wells that were landed in the Lower portion of the Upper Wolfcamp. The "reference" wells were the Middle Wolfcamp wells. The Upper Wolfcamp wells are typically targeted/landed in largely carbonate sections, which tends to yield long drill times. These carbonate sections are thought to be a natural barrier to vertical hydraulic fracture growth between the Upper and Middle Wolfcamp formations.

The objective the work in this chapter is to identify if the hydraulic fracture stimulation treatments broke through these carbonate sequences and may have communicated with the Wolfcamp B formation. For reference, a carbonate barrier exists at a TVD of 8950 ft which is about 100 ft away from the landing points of the Lower Wolfcamp A wells and 50 ft above the Wolfcamp B wells.

The input data for the hydraulic fracture model are given in **Table 6.1**.

Table 6.1 — Fracture Model Properties.

Property	Value
Porosity (fraction)	0.06
TVD at Pore Pressure (ft)	8860
Fluid Gradient (psi/ft)	0.59
Water Saturation (fraction)	0.65
Oil Specific Gravity (deg API)	42
Gas Specific Gravity (Air = 1)	0.8
Reservoir Temperature (Deg F)	180

For this work, the reference well is a Wolfcamp B well and the treatment well was a Lower Wolfcamp A well. Based on the number Lower Wolfcamp A wells, there are three fracture models covering the first three stages per well. Additionally, the model assumes that fracture height growth will be symmetrical upward and downward.

6.2 Discussion of Results

As results, the minimum and maximum computed fracture heights are summarized in **Table 6.2**.

Table 6.2 — Computed Fracture Heights.

Well	Minimum Fracture Height (ft)	Maximum Fracture Height (ft)
3	30	180
7	20	290
11	20	295

Considering all of the Lower Wolfcamp A wells, Well 3 may not have fractured through the carbonate barrier during stage 3, and most likely, the remainder of the wells did fracture through the carbonate barrier during the toe stages. This may have caused communication between the Wolfcamp B wells, indicating the likelihood that these wells interfered/competed during flowback production. Well 13 is another Lower Wolfcamp A well that does not have post-job treatment data available and was not investigated.

Not all of the stages were modeled for all wells. The objective of this sub-study is to determine if the fracture modeling could reveal if the lower Wolfcamp A wells may have fractured through the carbonate barrier since this is the closest landing point to this barrier. It is assumed that the carbonate barrier could provide fracture containment between the Lower Wolfcamp A and the Wolfcamp B, but that may not be what actually happened.

A limitation of the fracture modeling is that there is an assumption of symmetrical height growth upward and downward from the well, which may not be realistic. However, fracture modeling does yield a good indication if the carbonate section is an effective barrier for fracture containment when fracturing the Lower Wolfcamp A wells.

Lastly, proppant embedment and proppant crushing are out of the scope of this work. Proppant crushing results from the proppant packing condition and the strength of proppant, while proppant embedment depends on both the mechanical properties of proppants and fracture surfaces (Wu et al 2017).

CHAPTER 7

SUMMARY, CONCLUSIONS, RECOMMENDATIONS

7.1 Summary

A practice-based workflow was conducted on an entire section of wells landed in two targets, covering three landing points — specifically, the upper portion of the Wolfcamp A, the Lower portion of Wolfcamp A, and the Wolfcamp B. Decline curve analyses, rate transient analyses, and pressure transient analysis were conducted to assess additional drawdown opportunities for wells that have been producing for at least six months. Reservoir modeling was also conducted for selected wells to explore the impact of drawdown opportunities — *i.e.*, the potential effects of increasing pressure drop (*i.e.*, drawdown) on the long-term performance (including EUR) for a given well. Lastly, fracture modeling was performed to investigate if the fracture network(s) for a given well could potentially overlap in a given multiwell development (*i.e.*, to assess interaction/interference of the fracture networks).

7.2 Conclusions

Decline curve analyses, rate transient analyses, and pressure transient analysis yield some salient conclusions regarding the existing drawdown strategies for the wells investigated.

Decline Curve Analyses — Wells landed in the lower portion of the Wolfcamp A have lower EUR's due to the small vertical distance between the Upper Wolfcamp A and the Upper Wolfcamp B ($\approx 100'$). With all of these wells on gas-lift, it seems that the upper Wolfcamp A wells are converging to higher minimum flowing bottomhole pressures than the Wolfcamp B wells, indicating that a more aggressive drawdown strategy may be plausible.

Rate Transient Analyses — Lower Wolfcamp A wells achieved the end of linear flow more quickly than wells in the Upper Wolfcamp A and the Upper Wolfcamp. Upper Wolfcamp A wells reach the end of linear flow much slower compared to the lower Wolfcamp B wells, suggesting additional drawdown opportunities. From this work, the Wolfcamp B wells had the shortest fracture half-lengths, suggesting that the vertical distance between the Lower Wolfcamp A and the Wolfcamp B may be too small to generate long fracture half-lengths. Calculated permeabilities appear to depend on the effectiveness of the stimulation for each well. The Upper Wolfcamp A and Upper Wolfcamp B wells tend to have higher permeabilities calculated from RTA matches.

Pressure Transient Analyses — The pressure derivative trends for the wells selected for pressure transient analysis (PTA) all appear to be heavily affected by load-up/wellbore storage at early times. In fact, it is not clear from the pressure drop and pressure drop derivative trends that these data are "analyzable" in a traditional sense. In particular, some wells exhibit significant artifacts, most likely due to the fact that these are "opportunity" shut-ins (*i.e.*, analysis of data taken during operational downtime as opposed to a specifically designed testing sequence). The kh -values estimated from the PTA data matches are much higher than those that were assumed for the RTA matches. In addition, the reservoir pressures are estimated to be lower compared to the DFIT pressure values used for RTA (DFITs are early time injection tests, where these are used to estimate fracture properties and initial reservoir pressure).

Numerical and Fracture Modeling — Using reservoir and fracture modelling, the same conclusions are drawn for the drawdown strategies for all of the cases considered in this work. Although intuitive, increasing the drawdown (*i.e.*, pressure drop) for all wells and all

conditions will yield the highest production rates and recovery. Regardless of the case considered, the majority of the oil recovery will occur during the early-time of the well life (within 3-5 years). Based on the completion designs, as considered in selected cases, there is evidence of early communication based on the fracture heights generated from the fracture treatment designs. However, based on modelling performed in this work, as long as high production rates can be achieved in the early-time portion of the well life, then such communication is observed to be negligible.

7.3 Recommendations

Based on the results obtained from this study, additional drawdown (*i.e.*, flow per unit pressure drop) is possible/probable to exist. Therefore, it is recommended that for a given well, operators should attempt to establish minimum flowing bottomhole pressure as soon as possible for wells in the Midland Basin Wolfcamp A and Wolfcamp B reservoirs.

NOMENCLATURE

DCA	=	Decline Curve Analysis
DFIT	=	Diagnostic Fracture Injection Test
RTA	=	Rate transient Analysis
PTA	=	Pressure Transient Analysis
h	=	Thickness (ft)
k	=	Permeability (md)
p_i	=	Initial reservoir pressure (psia)
s	=	Skin factor (dimensionless)
x_f	=	Fracture half-length (ft)
$\Delta\sigma_{closure}$	=	Fracture closure pressure (psia)
α	=	Biot's coefficient
ν	=	Poisson's Ratio
Δp_p	=	Pore pressure change (psi)

REFERENCES

- Andrews, J. S., Kittilsen, P., Låhne, T., and Antonsen, J. R. (2017, April 5). Optimizing Bean-Up Procedure after Well Shut-in. Simple Rock Mechanical Aspects and Operational Guidelines. Society of Petroleum Engineers. doi:10.2118/185906-MS
- Chhatre, S., Chen, A., Al-Rukabi, M., Berry, D., Longoria, R., Guice, K., & Maloney, D. (2019, July 31). Measurement of Gas-Oil Relative Permeability in Unconventional Rocks. Unconventional Resources Technology Conference. doi:10.15530/urtec-2019-313
- Collins, P., Ilk, D., and Blasingame, T. A. (2014, October 27). Practical Considerations for Forecasting Production Data in Unconventional Reservoirs — Variable Pressure Drop Case. Society of Petroleum Engineers. doi:10.2118/170945-MS
- Crespo, P. A., and Cuervo, S. (2018, August 14). Drawdown Management Optimization from Time-Lapse Numerical Simulation. Society of Petroleum Engineers. doi:10.2118/191828-MS
- Deen, T., Daal, J., and Tucker, J. (2015, September 28). Maximizing Well Deliverability in the Eagle Ford Shale Through Flowback Operations. Society of Petroleum Engineers. doi:10.2118/174831-MS
- Eltaher, E. K., Muradov, K., Davies, D. R., and Grebenkin, I. M. (2014, October 27). Autonomous Inflow Control Valves - their Modelling and Added Value; Society of Petroleum Engineers. doi:10.2118/170780-MS
- Kappa Engineering (2020) Citrine (Field Performance Analysis) Software, Kappa Engineering, Mougins, France.

Karantinos, E., Sharma, M. M., Ayoub, J. A., Parlar, M., and Chanpura, R. A. (2016, February 24). Choke Management Strategies for Hydraulically Fractured Wells and Frac-Pack Completions in Vertical Wells. Society of Petroleum Engineers. doi:10.2118/178973-MS

Kumar, A., Seth, P., Shrivastava, K., and Sharma, M. M. (2018, October 16). Optimizing Drawdown Strategies in Wells Producing from Complex Fracture Networks. Society of Petroleum Engineers. doi:10.2118/191419-18IHFT-MS

Lerza, A., Rojas, D., and Liang, B. (2018, August 9). Defining the Optimal Drawdown Strategy in the Vaca Muerta Formation. Unconventional Resources Technology Conference. doi:10.15530/URTEC-2018-2880115

Li, T., Chu, W., and Leonard, P. A. (2019, July 31). Analysis and Interpretations of Pressure Data from the Hydraulic Fracturing Test Site (HFTS). Unconventional Resources Technology Conference. doi:10.105530/urtec-2019-233

Rojas, D., and Lerza, A. (2018, March 13). Horizontal Well Productivity Enhancement through Drawdown Management Approach in Vaca Muerta Shale. Society of Petroleum Engineers. doi:10.2118/189822-MS

Shelokov, V., Sarkar, M., and Wydrinski, R. (2017, July 24). Geomechanical Facies Model for Wolfcamp Formation (Midland Basin). Unconventional Resources Technology Conference. doi:10.15530/URTEC-2017-2694220

Tompkins, D., Sieker, R., Koseluk, D., and Cartaya, H. (2016, August 1). Managed Pressure Flowback in Unconventional Reservoirs: A Permian Basin Case Study. Unconventional Resources Technology Conference. doi:10.15530/URTEC-2016-2461207

Wang, H., and Sharma, M. M. (2019, January 29). A Novel Approach for Estimating Formation Permeability and Revisit After-Closure Analysis from DFIT. Society of Petroleum Engineers. doi:10.2118/194344-MS

Wang, H., and Sharma, M. M. (2019, August 1). A Novel Approach for Estimating Formation Permeability and Revisiting After-Closure Analysis of Diagnostic Fracture-Injection Tests. Society of Petroleum Engineers. doi:10.2118/194344-PA

Wang, S., Tan, Y., Sangnimnuan, A., Khan, S., Liang, B., and Rijken, P. (2019, July 25). Learnings from the Hydraulic Fracturing Test Site (HFTS) #1, Midland Basin, West Texas - A Geomechanics Perspective. Unconventional Resources Technology Conference. doi:10.105530/urtec-2019-1570

Wilson, K., and Hanna Alla, R. R. (2017, July 24). Efficient Stress Characterization for Real-Time Drawdown Management. Unconventional Resources Technology Conference. doi:10.15530/URTEC-2017-2721192

Wilson, K., Ahmed, I., and MacIvor, K. (2016, August 1). Geomechanical Modeling of Flowback Scenarios to Establish Best Practices in the Midland Basin Horizontal Program. Unconventional Resources Technology Conference. doi:10.15530/URTEC-2016-2448089

Wu, W., Russell, R., & Sharma, M. (2017, July 24). An Experimental Method to Study the Impact of Fracturing Fluids on Fracture Conductivity in Heterogeneous Shales. Unconventional Resources Technology Conference. doi:10.15530/URTEC-2017-2669936